arXiv:2511.15689v4 [econ.EM] 20 Jul 2026

Semiparametric Estimation of Fractional Integration: An Evaluation of Local Whittle Methods

JASON R. BLEVINS

The Ohio State University

July 20, 2026

Abstract. Fractionally integrated time series, exhibiting long memory with slowly decaying autocorrelations, are frequently encountered in economics, finance, and related fields. Since the seminal work of Robinson (1995a), a variety of semiparametric local Whittle estimators have been proposed for estimating the memory parameter d, each with a distinct range of validity and different robustness properties, leaving applied researchers to decide which to use and under what conditions. This paper offers a practitioner's guide to six such estimators. Using a common Monte Carlo design, we map how each estimator behaves under short-run dynamics, unknown means, and time trends—the conditions under which each remains reliable and the characteristic way each breaks down. This reveals a tension between efficiency and robustness: the exact local Whittle estimator uniquely pairs the lowest asymptotic variance with an unrestricted parameter range, but requires the mean and trend to be handled with care. We then illustrate these failure modes, along with the difficulties introduced by structural breaks, on several macroeconomic, financial, and climate time series, where a naïvely applied estimator can report near-stationarity for a series that better-matched methods identify as strongly nonstationary. The resulting guidance on estimator choice and bandwidth selection is anchored by exact reproductions of published results from this literature, along with open source replication code and datasets.

Keywords: fractional integration, long memory, nonstationarity, semiparametric estimation, local Whittle estimation, exact local Whittle estimation.

JEL Classification: C13, C14, C22, C52.

1. Introduction

Applied researchers who estimate the memory parameter d of a fractionally integrated series often encounter an uncomfortable fact: different semiparametric estimators, applied to the same data, can disagree sharply. For French inflation (log-differenced CPI on an extended 1955–2025 sample), the six estimators we consider yield full-sample estimates $\hat{d}$ from 0.12 to 0.80, a range that includes the nonstationarity boundary at 0.50 and leads to opposite conclusions about persistence. For U.S. industrial production (log monthly index), the

exact local Whittle (ELW) estimator yields $\hat{d} = 0.10$, implying behavior close to $I(0)$, while tapered estimators yield $\hat{d} \approx 1.3$, implying strong nonstationarity. Disagreements like these may reflect estimator limitations, features of the data, or statistical uncertainty about d. The goal of this paper is to evaluate these estimators and, in doing so, to show practitioners how to identify such issues and how to correct them.

The memory parameter is of interest in many fields such as macroeconomics, finance, and climate econometrics. A primary reason to estimate d, rather than simply difference or detrend a series, is to preserve information for forecasting. The hyperbolic decay of a long-memory process's autocovariances carries predictive content at horizons where covariance-stationary short-memory models do not (Bhardwaj and Swanson, 2006). The same consideration motivates the use of fractional differencing in financial machine learning, to render a series stationary for predictive modeling while preserving as much memory as possible (López de Prado, 2018).

Since the seminal work of Granger and Joyeux (1980) and Hosking (1981), who introduced fractionally integrated processes to model intermediate persistence between stationary and unit-root behavior, an extensive literature on semiparametric estimation of d has emerged. For a broad survey of long memory and fractional integration in econometrics, see Baillie (1996). The early contributions of Geweke and Porter-Hudak (1983) and Robinson (1995b) developed log-periodogram regressions for frequency-domain estimation of d. Alternatively, by maximizing a quasi-likelihood function based on the Whittle likelihood, the local Whittle (LW) estimator of Künsch (1987) and Robinson (1995a) attains the conjectured[1] asymptotic variance lower bound of $1/4$ for stationary processes with $d \in (-1/2, 1/2)$.

Velasco (1999) and Hurvich and Chen (2000) developed tapered LW variants that extended the method to nonstationary processes, but at the cost of efficiency. Shimotsu and Phillips (2005) introduced the ELW estimator, which restored efficiency through exact fractional differencing while extending the method to the entire parameter space. The two-step ELW (2ELW) procedure of Shimotsu (2010) further extended the approach to processes with unknown means and time trends. The modified local Whittle estimator of Hou and Perron (2014) (LWLFC) provided robustness to low-frequency contamination such as level shifts.

Other work has extended the scope of local Whittle methods along several dimensions: to a wider memory range via a generalized discrete Fourier transform (Abadir, Distaso, and Giraitis, 2007), to reduced bias in the presence of short-run dynamics (Robinson and Henry, 2003; Andrews and Sun, 2004), to multiple poles at seasonal and cyclical frequencies (Arteche, 2020; Wingert, Leschinski, and Sibbertsen, 2020), to perturbed fractional processes

[1] Robinson (1995a, p. 1640) conjectured that the semiparametric efficiency bound for this class of estimators is $1/4$. Although no estimator has achieved lower asymptotic variance, the semiparametric efficiency bound has not been formally established.

(Frederiksen, Nielsen, and Nielsen, 2012), and to fractional cointegration (Nielsen, 2007; Shimotsu, 2012).

Previous authors have carried out finite-sample comparison studies that provide a foundation for our work. Nielsen and Frederiksen (2005) conducted an extensive Monte Carlo comparison of parametric, semiparametric, and wavelet estimators. Among bias-reducing semiparametric estimators, they found that the local polynomial Whittle estimator of Andrews and Sun (2004) and the bias-reduced log-periodogram regression of Andrews and Guggenberger (2003) substantially reduced bias in the presence of persistent short-run dynamics, at the cost of increased variance. A related study by García-Enríquez and Hualde (2019) compared standard local Whittle estimation with the bias-reducing variants of Robinson and Henry (2003) and Andrews and Sun (2004). They found that the benefits depend on the nature of the underlying short-run dynamics. These methods are helpful for moderate autoregressive short-run dynamics, but they can underperform the simpler standard LW estimator when short-run dynamics are mild.

Two features separate the present study from this earlier work. First, neither assembles the full set of estimators compared here: Nielsen and Frederiksen (2005) include a feasible exact local Whittle estimator alongside the standard LW estimator, but the Hurvich–Chen-tapered LW estimator of Hurvich and Chen (2000), the two-step ELW estimator of Shimotsu (2010), and the LWLFC estimator of Hou and Perron (2014)—methods that accommodate unknown means, trends, and level shifts—are included in neither comparison. Second, neither extends the comparison beyond simulations into empirical applications that connect the estimators to failures a practitioner can diagnose in a specific series.

This paper addresses these gaps with a unified, practitioner-oriented comparison of existing local Whittle estimators. Our contribution is threefold. First, we compare the finite-sample performance of six estimators across an expanded parameter range: the standard LW, Velasco-tapered LW, and ELW estimators, together with three methods not previously included in such a comparison—the Hurvich–Chen-tapered LW, two-step ELW, and LWLFC estimators. To validate our implementations, we independently reproduce key published Monte Carlo results for these estimators before extending them in a unified design, with complete open-source replication materials provided for every result.[2]

Second, we use the simulations to document the characteristic failure modes of each estimator: the conditions—persistent short-run dynamics, an unknown mean, a time trend, or nonstationarity beyond a method's valid range—under which it becomes unreliable, and the nature of its breakdown. The ELW estimator illustrates this: it attains an asymptotic variance one-third that of a higher-order tapered LW estimator, but requires the mean to

[2]All replication code and datasets are available at `https://github.com/jrblevin/lws`, and all estimates were computed using PyELW (Blevins, 2026), a Python library for local Whittle estimation.

be handled correctly, and the ideal correction depends on the memory parameter itself, a difficulty that the two-step variant mitigates.

Third, through a series of empirical case studies, we show these failure modes arising in practice and how to diagnose them. For U.S. industrial production, the ELW objective function produces a spurious global minimum near $d = 0.1$, while 2ELW's adaptive mean correction reshapes the objective so that its minimum is near the persistent value obtained by other estimators. For French inflation, a series where genuine long memory and structural breaks coexist, level shifts inflate the standard and tapered estimates. A unified comparison reveals patterns of agreement and disagreement that often point to the data feature responsible. We offer this as informal guidance rather than a formal procedure, distilling from these cases practical lessons for estimator choice given the features one has reason to suspect in the data.

The remainder of this paper is organized as follows. Section 2 reviews the theoretical development of local Whittle estimation methods and reports our replications of several main results from the literature for each method. Section 3 presents a new, cross-method Monte Carlo comparison with controlled contaminations. Section 4 presents our extended empirical analyses based on several macroeconomic, financial, and climate time series. Section 5 summarizes our guidance on selecting and applying local Whittle methods in practice. Section 6 concludes.

2. Local Whittle Estimators

In this section, we briefly review six major local Whittle estimators. We also independently reproduce key Monte Carlo results from Shimotsu and Phillips (2005) and Shimotsu (2010).[3] Consider the fractionally integrated process X_t defined as

$$(1) \quad (1-L)^{d_0} X_t = u_t \, 1\{t \geq 1\}, \quad t = 0, \pm 1, \pm 2, \ldots,$$

where L is the lag operator, $d_0 \in \mathbb{R}$ denotes the true memory parameter, $1\{\cdot\}$ denotes the indicator function, and u_t is a stationary, mean-zero process with spectral density $f_u(\lambda)$. Equation (1) is solved under the initialization $X_t = 0$ for $t \leq 0$, which uniquely determines X_t for $t \geq 1$.[4] The memory parameter d_0 determines the fundamental properties of X_t: $I(0)$ behavior when $d_0 = 0$, stationary long memory for $d_0 \in (0, 1/2)$, nonstationary but mean-reverting dynamics for $d_0 \in [1/2, 1)$, and the unit-root case when $d_0 = 1$. Negative

[3] The Original and Replication columns in each panel of Tables 1 and 2 allow direct comparison and agree to within a few thousandths in most cells. The larger differences occur mainly at extreme parameters (e.g., $d = \pm 3.5$), far outside the estimators' valid ranges.

[4] The process defined in (1) is a "Type II" process, as opposed to a "Type I" process, which applies the filter to a doubly-infinite sequence.

values of d_0 generate antipersistent processes, while $d_0 > 1$ yields nonstationary processes that are not mean-reverting.

The estimators we consider are frequency-domain methods that exploit the distinctive spectral properties of long-memory processes without specifying a parametric functional form for $f_u(\lambda)$. The Whittle likelihood (Whittle, 1951) provides a computationally efficient approximation to the Gaussian likelihood by working in the frequency domain, where the discrete Fourier coefficients are asymptotically independent complex normal random variables (Brillinger, 1981, Theorem 4.4.1). By focusing on low-frequency behavior, where the memory parameter dominates the shape of the spectral density, local Whittle methods offer two advantages: they avoid both the computationally intensive matrix inversion required by time-domain maximum likelihood and the need for a complete parametric specification.

2.1. Local Whittle Estimation

The local Whittle estimator of Robinson (1995a) exploits the power-law behavior of the spectral density near zero:

$$f_X(\lambda) \sim G\lambda^{-2d_0} \quad \text{as} \quad \lambda \to 0^+, \tag{2}$$

where $a \sim b$ means that $a/b \to 1$ and $G = f_u(0) > 0$.[5] This relationship captures the quintessential long-memory properties while remaining agnostic about the specific parametric form of the short-run dynamics.

The LW approach restricts attention to the first $m = m(n) \ll n$ Fourier frequencies where (2) holds most accurately, avoiding contamination from short-run dynamics at higher frequencies. We define the discrete Fourier transform of a_t at frequencies $\lambda_j = 2\pi j/n$ as

$$w_a(\lambda_j) = \frac{1}{\sqrt{2\pi n}} \sum_{t=1}^{n} a_t e^{it\lambda_j}.$$

Let $I_a(\lambda_j) = |w_a(\lambda_j)|^2$ denote the periodogram. The Whittle approximation to the (negative) Gaussian log-likelihood is

$$\sum_{j=1}^{m} \left[\log f_X(\lambda_j) + \frac{I_X(\lambda_j)}{f_X(\lambda_j)} \right].$$

Substituting the power-law approximation $f_X(\lambda_j) \approx G\lambda_j^{-2d}$ for the unknown spectral density

[5] For nonstationary processes with $d_0 \geq 1/2$, the classical spectral density is undefined due to infinite variance. In this case, $f_X(\lambda)$ is interpreted as a pseudo-spectral density.

and concentrating out the nuisance parameter G yields the local Whittle objective function:

$$R(d) = \log\left(\frac{1}{m}\sum_{j=1}^{m}\lambda_j^{2d} I_X(\lambda_j)\right) - \frac{2d}{m}\sum_{j=1}^{m}\log\lambda_j. \tag{3}$$

The local Whittle estimator is defined as:

$$\hat{d}_{\mathrm{LW}} = \underset{d\in[\Delta_1,\Delta_2]}{\arg\min}\ R(d),$$

where $[\Delta_1, \Delta_2]$ denotes the admissible parameter space. Since the periodogram $I_X(\lambda_j)$ does not depend on d, it can be precomputed from the data and so the objective function requires only $O(m)$ operations per evaluation. The objective function $R(d)$ is also convex in d (Baum, Hurn, and Lindsay, 2020, Appendix A), meaning that any local minimum reached by an optimization algorithm is also the global minimum. Robinson (1995a) established regularity conditions under which for $d_0 \in (-1/2, 1/2)$, the local Whittle estimator is asymptotically normal:

$$\sqrt{m}(\hat{d}_{\mathrm{LW}} - d_0) \xrightarrow{\mathrm{d}} \mathrm{N}\left(0, 1/4\right). \tag{4}$$

The asymptotic variance of $1/4$ implies an asymptotic standard error of $1/\sqrt{4m}$ for $\hat{d}_{\mathrm{LW}}$. Velasco (1999) extended this analysis into the nonstationary region, showing that the estimator remains consistent for $d_0 \in (-1/2, 1)$ and asymptotically normal for $d_0 \in (-1/2, 3/4)$.

The bandwidth parameter m controls the bias-variance trade-off. Increasing m includes more frequencies which reduces variance, but this increases bias since higher frequencies are influenced more by short-run dynamics. Henry and Robinson (1996) show that the theoretical optimal rate is $m \propto n^{4/5}$, which minimizes the mean squared error (MSE) of the estimator. However, this rate can be sensitive to model misspecification and short-run dynamics, leading practitioners to often use more conservative choices $m = \lfloor n^{\alpha} \rfloor$ with $\alpha < 4/5$. See Henry (2001), Baillie, Kapetanios, and Papailias (2014), and particularly the discussion in Arteche and Orbe (2017) for further developments on bandwidth selection, which we revisit in Section 4.

Table 1 collects our replications of Monte Carlo results, demonstrating the finite-sample properties of the standard LW estimator and tapered variants (introduced below), with one panel per method. These panels replicate Tables 1 and 2 of Shimotsu and Phillips (2005). Each sample consists of $n = 500$ simulated observations from an ARFIMA$(0, d, 0)$ process. The table shows the bias, standard deviation, and mean squared error of the estimates over 10,000 replications. The number of frequencies used was $m = \lfloor n^{0.65} \rfloor = 56$. The "Original" columns report the published results while the "Replication" columns show the independent

TABLE 1. Replication of Published Monte Carlo Results: LW and Tapered LW Estimators

	Original			Replication		
d	Bias	S.D.	MSE	Bias	S.D.	MSE
Panel A: Local Whittle (LW)						
−1.3	0.4109	0.2170	0.2160	0.4114	0.2182	0.2169
−0.7	0.0353	0.0885	0.0091	0.0373	0.0882	0.0092
−0.3	−0.0027	0.0781	0.0061	−0.0008	0.0780	0.0061
0.0	−0.0075	0.0781	0.0062	−0.0060	0.0775	0.0060
0.3	−0.0066	0.0785	0.0062	−0.0060	0.0778	0.0061
0.7	0.0099	0.0812	0.0067	0.0095	0.0812	0.0067
1.3	−0.2108	0.0982	0.0541	−0.2106	0.0986	0.0541
Panel B: Velasco tapered LW, Bartlett taper						
−3.5	1.6126	0.3380	2.7148	1.6231	0.3326	2.7450
−2.3	0.2155	0.1726	0.0762	0.2173	0.1734	0.0773
−1.7	0.0259	0.1235	0.0159	0.0279	0.1211	0.0154
−1.3	0.0081	0.1211	0.0147	0.0090	0.1203	0.0146
−0.7	−0.0068	0.1219	0.0149	−0.0048	0.1200	0.0144
−0.3	−0.0133	0.1224	0.0151	−0.0097	0.1201	0.0145
0.0	−0.0138	0.1224	0.0152	−0.0111	0.1201	0.0145
0.3	−0.0132	0.1235	0.0154	−0.0103	0.1201	0.0145
0.7	−0.0068	0.1227	0.0151	−0.0051	0.1203	0.0145
1.3	0.0140	0.1232	0.0154	0.0170	0.1222	0.0152
1.7	0.0456	0.1288	0.0187	0.0485	0.1258	0.0182
2.3	−0.1781	0.1419	0.0519	−0.1774	0.1410	0.0514
3.5	−1.4541	0.1338	2.1322	−1.4529	0.1378	2.1298
Panel C: Hurvich–Chen tapered LW (HC)						
−3.5	2.5889	0.3037	6.7946	2.5920	0.2988	6.8075
−2.3	1.1100	0.2893	1.3157	1.1104	0.2882	1.3160
−1.7	0.4474	0.2154	0.2466	0.4493	0.2149	0.2481
−1.3	0.1551	0.1231	0.0392	0.1547	0.1239	0.0393
−0.7	0.0278	0.0957	0.0099	0.0294	0.0959	0.0101
−0.3	0.0100	0.0971	0.0095	0.0134	0.0972	0.0096
0.0	0.0034	0.0985	0.0097	0.0053	0.0978	0.0096
0.3	−0.0033	0.1004	0.0101	−0.0007	0.0983	0.0097
0.7	−0.0066	0.0994	0.0099	−0.0055	0.0983	0.0097
1.3	−0.0079	0.0987	0.0098	−0.0050	0.0974	0.0095
1.7	0.0008	0.0972	0.0095	0.0029	0.0957	0.0092
2.3	0.0528	0.0981	0.0124	0.0557	0.0981	0.0127
3.5	−0.4079	0.1142	0.1795	−0.4069	0.1144	0.1787

Notes: Bias, standard deviation, and mean squared error of the estimates over 10,000 replications, each with $n = 500$ observations from ARFIMA$(0, d, 0)$ and $m = \lfloor n^{0.65} \rfloor = 56$ frequencies. "Original" columns report published values: Panel A from the right panel of Table 1 of Shimotsu and Phillips (2005), and Panels B and C from the right and left panels of their Table 2. "Replication" columns report results from our Python implementation.

results from our Python implementation.

Panel A contains the results for the LW estimator for a range of d values. Within the stationary and invertible range $d \in (-1/2, 1/2)$, the estimator has very little bias, standard deviations of about 0.078 (moderately above the theoretical asymptotic value of $1/\sqrt{4m} = 0.067$ due to the small bandwidth), and low mean squared errors. However, the theoretical limitations are apparent for the more extreme values $d = -1.3$ and $d = 1.3$, where validity breaks down and bias dominates the mean squared error.

2.2. Extending the Range via Tapering

The LW estimator achieves asymptotic normality over the range $d_0 \in (-1/2, 3/4)$ with asymptotic variance $1/4$; however, estimation outside of this limited range or in the presence of deterministic components requires a different approach. To address this limitation, Velasco (1999) (V) developed a class of tapered LW estimators that trades efficiency for a wider validity range.

Formally, tapering involves weighting the original series X_t by a sequence h_t that is symmetric around $\lfloor n/2 \rfloor$, with $\max_t h_t = 1$, and that decays smoothly to zero at the sample boundaries. The tapered periodogram

$$I_h(\lambda_j) = |w_h(\lambda_j)|^2, \quad w_h(\lambda_j) = \frac{1}{\sqrt{2\pi n}} \sum_{t=1}^{n} h_t X_t e^{it\lambda_j},$$

replaces the standard periodogram $I_X(\lambda_j)$ in the objective function. Because the periodogram treats the sample as repeating, a nonstationary series creates an artificial jump between its two ends that contaminates low frequencies (the very frequencies that identify d_0). Tapering the ends of the series removes it. For Velasco tapers, the periodogram uses subsampled frequencies $\lambda_j = 2\pi j/n$ with $j = p, 2p, 3p, \ldots, m$, where p is the taper order. As with the standard LW estimator, evaluating these tapered objective functions remains computationally inexpensive and the criterion functions are amenable to simple scalar minimization algorithms.

Using tapers of higher orders p extends the valid range of d_0 values and provides robustness to trends of order $p-1$. The triangular Bartlett window taper ($p = 2$) is valid for $d_0 \in (-1/2, 3/2)$ and robust to linear trends, while the Zhurbenko–Kolmogorov (henceforth Kolmogorov) taper ($p = 3$) is valid for $d_0 \in (-1/2, 5/2)$ and robust to linear and quadratic time trends. However, as mentioned, this robustness is at the expense of increased variance. The variance of the limiting distribution of the tapered LW estimator is $p\Phi_p/4$, where Φ_p is a constant that depends on the order p of the taper.[6] For $p = 2$ with $\Phi_2 = 1.05000$, the

[6]The limiting distribution and corresponding numerical constants are given in Theorem 6 of Velasco (1999).

asymptotic variance is $2 \times 1.05 = 2.1$ times the LW variance; for $p = 3$ with $\Phi_3 = 1.00354$, the variance is 3.01 times the LW variance.

Panel B of Table 1 replicates the right panel of Table 2 from Shimotsu and Phillips (2005) to illustrate the finite-sample behavior of the Bartlett-tapered LW estimator of Velasco (1999). Within the range $d \in [-1.7, 1.7]$ (which even includes values far outside the method's valid range), the estimates have low bias and standard deviations of around 0.120, roughly 25% above the asymptotic value of $\sqrt{2.1/4m} = 0.097$. As expected, at more extreme values of d outside the method's valid range, we see large biases and mean squared errors.

In Appendix B, we compare the finite-sample performance of all three tapers considered by Velasco (1999). The comparison reflects the fundamental trade-off between bias and variance due to tapering: the Bartlett taper achieves the lowest variance, while the order-three Kolmogorov taper retains low bias much deeper into the nonstationary range. In the cross-method comparisons that follow, we use the Kolmogorov taper for its wider range of validity.

2.3. Efficiency Gains via Complex-Valued Tapering

Hurvich and Chen (2000) (HC) developed an alternative tapered local Whittle estimator based on applying a complex-valued taper $h_t = \frac{1}{2}\left(1 - e^{i2\pi(t-1/2)/n}\right)$, defined in their equation (3), to first-differenced data $\Delta X_t = X_t - X_{t-1}$. The HC-tapered LW estimator extends the valid range to $d_0 \in (-1/2, 3/2)$ while achieving lower variance than Velasco tapers. It is also robust to linear trends, due to first-differencing the data before applying the taper. After estimating the memory parameter of the differenced data, the researcher adds back one degree of integration to the resulting estimate. Because the tapered Fourier transform combines two adjacent untapered ordinates, the HC method evaluates the spectrum at the shifted frequencies $\lambda_{\tilde{j}} = 2\pi(j + 0.5)/n$. The estimator is defined as

$$\hat{d}_{\mathrm{HC}} = 1 + \underset{d \in [\Delta_1 - 1, \Delta_2 - 1]}{\arg\min} R_{\mathrm{HC}}(d),$$

where $R_{\mathrm{HC}}(d)$ has the same form as $R(d)$, but uses the tapered periodogram of ΔX_t. The asymptotic variance of the HC estimator is $1.5/4$, which is higher than $1/4$ for the LW estimator, but lower than $2.1/4$ when using a second-order Velasco taper.

In Panel C of Table 1, we replicate the HC-tapered LW estimator results from Shimotsu and Phillips (2005, Table 2). The HC estimator shows good finite-sample performance in its valid range $d \in (-1/2, 3/2)$ and beyond, with degradation at more extreme values. We defer a full cross-method comparison until Section 3.

2.4. Exact Local Whittle Estimation

The standard local Whittle estimator assumes that the power-law relationship between the periodograms of the observed and unobserved processes—$I_u(\lambda_j) \approx \lambda_j^{2d_0} I_X(\lambda_j)$—holds for frequencies near zero. This approximation is valid when $|d_0| < 1/2$. The exact local Whittle (ELW) estimator of Shimotsu and Phillips (2005) instead works directly with fractionally differenced data, avoiding this approximation. From the model in (1), we see that the periodogram of the fractionally differenced series $\Delta^d X_t \equiv (1-L)^d X_t$ equals the periodogram of u_t precisely when $d = d_0$, regardless of the value of d_0. By fractionally differencing the series for each candidate d value during optimization, the ELW estimator removes the approximation error from the LW approach, extending consistency and asymptotic normality to the full parameter space.

The fractional differencing operator is defined by the binomial expansion

$$\Delta^d X_t = \sum_{k=0}^{t-1} \pi_k(d) X_{t-k},$$

where the coefficients $\pi_k(d)$ can be computed using the recurrence

$$\pi_0(d) = 1, \quad \pi_k(d) = \pi_{k-1}(d) \cdot \frac{k-1-d}{k}, \quad k \geq 1.$$

This operator transforms the data to remove d orders of integration, and when $d = d_0$, this operation recovers the short-memory process u_t exactly.

The ELW objective function has a similar functional form as (3) for LW, but is based on the periodogram $I_{\Delta^d X}(\lambda_j)$ of the fractionally differenced series:

$$R_{\mathrm{ELW}}(d) = \log\left(\frac{1}{m}\sum_{j=1}^{m} I_{\Delta^d X}(\lambda_j)\right) - \frac{2d}{m}\sum_{j=1}^{m}\log\lambda_j. \tag{5}$$

Unlike for the LW objective, the periodogram $I_{\Delta^d X}(\lambda_j)$ must be recomputed for each candidate d. This introduces a nonlinear dependence on d and, as a result, the ELW objective is not guaranteed to be convex.

The primary advantage of the ELW estimator is that it remains valid whether d_0 lies in the stationary region or far in the nonstationary region, provided that the width of the optimization interval is at most $9/2$.[7] Despite this, the ELW estimator retains the same

[7]The width restriction arises because the proof of consistency requires different techniques when $|d - d_0| > 1/2$, which have been established only for $|d - d_0| \leq 9/2$. See the discussion on pp. 1894–1895 of Shimotsu and Phillips (2005) for details.

TABLE 2. Replication of Published Monte Carlo Results: Exact Local Whittle Estimators

	Original			Replication		
d	Bias	S.D.	MSE	Bias	S.D.	MSE
Panel A: Exact local Whittle (ELW)						
−3.5	−0.0024	0.0787	0.0062	−0.0014	0.0777	0.0060
−2.3	−0.0020	0.0774	0.0060	−0.0015	0.0777	0.0060
−1.7	−0.0020	0.0776	0.0060	−0.0015	0.0778	0.0061
−1.3	−0.0014	0.0770	0.0059	−0.0015	0.0778	0.0061
−0.7	−0.0024	0.0787	0.0062	−0.0015	0.0778	0.0061
−0.3	−0.0033	0.0777	0.0060	−0.0015	0.0779	0.0061
0.0	−0.0029	0.0784	0.0061	−0.0016	0.0778	0.0061
0.3	−0.0020	0.0782	0.0061	−0.0015	0.0779	0.0061
0.7	−0.0017	0.0777	0.0060	−0.0015	0.0778	0.0061
1.3	−0.0014	0.0781	0.0061	−0.0014	0.0779	0.0061
1.7	−0.0025	0.0780	0.0061	−0.0014	0.0778	0.0061
2.3	−0.0026	0.0772	0.0060	−0.0012	0.0779	0.0061
3.5	−0.0016	0.0770	0.0059	−0.0013	0.0778	0.0061
Panel B: Two-step exact local Whittle (2ELW)						
0.0	−0.0022	0.0762	0.0058	−0.0019	0.0758	0.0057
0.4	0.0001	0.0762	0.0058	0.0053	0.0814	0.0067
0.8	−0.0003	0.0762	0.0058	−0.0012	0.0764	0.0058
1.2	−0.0006	0.0755	0.0057	−0.0014	0.0778	0.0060

Notes: Bias, standard deviation, and mean squared error of the estimates over 10,000 replications of ARFIMA$(0, d, 0)$. "Original" columns report published values; "Replication" columns report results from our Python implementation. Panel A replicates the left panel of Table 1 of Shimotsu and Phillips (2005), with $n = 500$ and $m = 56$. Panel B replicates Table 2 of Shimotsu (2010), with $n = 512$ and $m = 57$.

asymptotic distribution as the LW estimator:

$$\sqrt{m}(\hat{d}_{\mathrm{ELW}} - d_0) \xrightarrow{\mathrm{d}} \mathrm{N}\left(0, 1/4\right).$$

The computational cost of ELW estimation is higher than for LW. The latter only required one precomputed periodogram calculation and no fractional differencing. For the ELW estimator, for each candidate value of d encountered during optimization, one needs to recompute the fractional difference $\Delta^d X_t$ and the corresponding periodogram $I_{\Delta^d X}$. While computing $\Delta^d X_t$ naïvely requires $O(n^2)$ operations, the fast fractional differencing algorithm of Jensen and Nielsen (2014), based on the fast Fourier transform, reduces this to $O(n \log n)$. The computational burden of ELW is therefore $O(n \log n)$ per objective function evaluation, as compared to $O(m)$ for LW. For this additional cost, we obtain a consistent estimator with asymptotic variance $1/4$ across the full parameter space.

Panel A of Table 2 presents our replication of the left panel of Table 1 from Shimotsu and Phillips (2005), demonstrating the finite-sample performance of the ELW estimator over an extended range of d values spanning $d \in [-3.5, 3.5]$. The results highlight the primary advantage of the ELW estimator: under ideal conditions, it exhibits minimal bias, standard deviations of about 0.078, and uniformly low mean squared errors for any value of d.

2.5. Robustness to Unknown Mean and Trend

The ELW estimator assumes that the stochastic process X_t has zero mean and does not contain a trend. However, real economic time series may have nonzero means and time trends. This led Shimotsu (2010) to develop the two-step exact local Whittle (2ELW) estimator, which addresses both issues while preserving the $\mathrm{N}(0, 1/4)$ limiting distribution, although with a limited parameter range. The valid range depends on whether a trend is included or not, as we will discuss below.

First, consider the model with an unknown mean:

$$X_t = \mu_0 + X_t^0, \quad X_t^0 = (1-L)^{-d_0} u_t \, 1\{t \geq 1\},$$

where μ_0 is an unknown constant. The problem this introduces is subtle. The best way to handle the mean depends on the unknown value of d_0 itself. For stationary processes ($|d_0| < 1/2$), the sample average $\hat{\mu} = \bar{X}$ is a reasonable estimator for μ_0. For nonstationary, highly persistent processes ($d_0 \geq 1/2$), the first observation $\hat{\mu} = X_1$ is a better estimator. To address this indeterminacy, Shimotsu (2010) proposed an adaptive mean estimator $\tilde{\mu}(d)$ and a modified ELW objective function based on fractionally differencing the mean-corrected data $X_t - \tilde{\mu}(d)$. The estimator $\tilde{\mu}(d)$ is based on a weight function that varies smoothly with the value of d:

$$\tilde{\mu}(d) = w(d)\bar{X} + (1 - w(d))X_1,$$

where $w(d)$ is the weight function

$$w(d) = \begin{cases} 1 & \text{if } d \leq \frac{1}{2}, \\ \frac{1}{2}[1 + \cos(4\pi d)] & \text{if } \frac{1}{2} < d < \frac{3}{4}, \\ 0 & \text{if } d \geq \frac{3}{4}. \end{cases} \tag{6}$$

The intuition behind this weighting is as follows: $w(d) = 1$ for stationary processes, so $\bar{X}$ receives full weight. ELW with $\hat{\mu} = \bar{X}$ remains consistent for $d_0 < 1$, but it loses asymptotic normality for $d_0 \geq 3/4$. Using X_1 instead extends asymptotic normality to $d_0 < 2$, so

$w(d) = 0$ for $d \geq 3/4$, placing full weight on X_1. The weight function incorporates a smooth cosine transition between these two extremes.

Estimation of the mean in this way significantly complicates the asymptotic theory, so Shimotsu (2010) proposed a two-step approach based on a $\sqrt{m}$-consistent first-step estimator. The first step applies one of the tapered LW estimators discussed above to obtain an initial estimate $\hat{d}_T$. The second step applies a single Newton–Raphson step to the modified ELW objective function starting from $\hat{d}_T$. Shimotsu (2010) noted that the Newton–Raphson step can become numerically unstable when the Hessian $R''(\hat{d}_T)$ takes very small values, resulting in extremely large updates, and recommended using $\max\{R''(\hat{d}_T), 2\}$ instead of the actual Hessian. The lower bound avoids extremely large steps leading to extreme estimates $\hat{d}_{\text{2ELW}}$.

For data believed to contain a polynomial trend of order k, the procedure first removes the trend via an OLS regression of X_t on $(1, t, t^2, \ldots, t^k)$, and then applies the above two-step procedure to the residuals. Shimotsu (2010) shows that the 2ELW estimator is consistent with detrending, but the valid parameter range is restricted to $d_0 \in (-1/2, 7/4)$, compared to $d_0 \in (-1/2, 2)$ for the unknown mean case. The procedure achieves the same $\text{N}(0, 1/4)$ limiting distribution as LW within these ranges while maintaining robustness to both unknown means and polynomial trends.

Panel B of Table 2 presents our replication of the 2ELW Monte Carlo results from Table 2 of Shimotsu (2010), which used $n = 512$ observations and $m = 57$ frequencies. The 2ELW estimator maintains good finite-sample properties, with minimal bias and performance that remains stable across the stationary ($d = 0.0, 0.4$) and nonstationary ($d = 0.8, 1.2$) regions. Here we only consider specifications for which there are no short-run dynamics ($\rho = 0$), but in Section 3 we investigate the robustness of 2ELW and other estimators in a more thorough set of benchmarks including cases with AR(1) short-run dynamics ($\rho > 0$), unknown means, and time trends.

2.6. Robustness to Low-Frequency Contamination

In practice, time series may be contaminated by level shifts that distort the spectrum at low frequencies. Diebold and Inoue (2001) and Granger and Hyung (2004) showed that such contaminations can manifest as spurious long memory. To address this, Hou and Perron (2014) developed a modified local Whittle estimator designed to be robust to low-frequency contamination (LWLFC) such as random level shifts, deterministic level shifts, and certain types of normalized trends of the form $h(t/n)$, which remain bounded as t grows. However, LWLFC is only valid for stationary processes with $d_0 \in [0, 1/2)$, and it remains sensitive to deterministic linear trends (Section 3.4).[8]

[8]Because of its specialized role and restricted range, LWLFC does not appear in every comparison below. We include it in the comprehensive Monte Carlo study (Section 3.1) and the structural-break application

Specifically, let Y_t denote the observed time series, which is assumed to follow

$$Y_t = \mu_0 + X_t + L_t,$$

where μ_0 is a constant, X_t is a fractionally integrated process with memory parameter d_0 as in (1), and L_t captures low-frequency disturbances.

The estimator introduces an additional parameter $\theta \geq 0$, representing a contamination ratio: the variance of the low-frequency contamination L_t relative to that of the long-memory component X_t. The modified objective function is

$$J(d, \theta) = \log\left(\frac{1}{m}\sum_{j=1}^{m}\frac{I_Y(\lambda_j)}{g_j}\right) + \frac{1}{m}\sum_{j=1}^{m}\log(g_j),$$

where $g_j = \lambda_j^{-2d} + \theta\lambda_j^{-2}/n$. The term $\theta\lambda_j^{-2}/n$ corrects the spectral density for the contribution of the low-frequency contamination. The LWLFC estimator is defined as

$$(\hat{d}_{\text{LWLFC}}, \hat{\theta}_{\text{LWLFC}}) = \underset{(d,\theta)\in[0,1/2)\times[0,\infty)}{\arg\min} J(d, \theta).$$

Hou and Perron (2014) state regularity conditions for which the LWLFC estimator is consistent and asymptotically normal with

$$\sqrt{m}(\hat{d}_{\text{LWLFC}} - d_0) \xrightarrow{\text{d}} \text{N}\left(0, 1/4\right).$$

The asymptotic variance is the same as that of the standard LW estimator, meaning that accounting for low-frequency contamination does not reduce efficiency, only range. If there is no contamination, then $\hat{\theta}_{\text{LWLFC}} \xrightarrow{\text{p}} 0$ and the LWLFC estimator is asymptotically equivalent to the standard LW estimator.

3. Monte Carlo Comparisons Across Methods

In this section, we compare the finite-sample performance of the six local Whittle estimators across several data-generating processes. We consider the impact of short-run dynamics, unknown means, and time trends, each under varying degrees of fractional integration. Additionally, in Appendix A we consider robustness to the sample size, the form of the short-run dynamics, and the innovation distribution.

Our Monte Carlo specifications follow conventions established in the literature. We use a sample size of $n = 500$ with Gaussian innovations and bandwidth $m = \lfloor n^{0.65} \rfloor$. These choices

(Section 4.4), but omit it where the general-purpose estimators are the focus.

are consistent with the baseline specifications in Shimotsu and Phillips (2005), Shimotsu (2010), and Nielsen and Frederiksen (2005). Hurvich and Chen (2000) also used $n = 500$ and Gaussian innovations, but with bandwidth $m = \lfloor 0.25n^{0.80} \rfloor$. To focus on the performance of estimators without bandwidth variability, for now we use a fixed bandwidth rule. We will evaluate data-driven bandwidth choices in empirical applications later in Section 4.

3.1. Comprehensive Estimator Comparison with Short-Run Dynamics

To establish a baseline for cross-estimator comparison, we revisit the Monte Carlo design from Table I of Hurvich and Chen (2000). Their experiment used 500 replications of simulated ARFIMA$(1, d, 0)$ processes with AR(1) short-run dynamics (autoregressive parameter ρ), while we use 10,000 replications for greater precision. We use bandwidth $m = 56$ following the standard rule $m = \lfloor n^{0.65} \rfloor$ mentioned above.

We extend their original study by comparing all six estimators: LW, V = Velasco (Kolmogorov), HC = Hurvich–Chen, ELW, 2ELW, and LWLFC. Furthermore, we evaluate these estimators over a wider range of 33 parameter combinations

$$(d, \rho) \in \{-2.2, -1.8, -1.2, -0.6, -0.3, 0.0, 0.3, 0.6, 1.2, 1.8, 2.2\} \times \{0.0, 0.5, 0.8\}.$$

This allows for a more thorough evaluation across ranges of fractional integration from strongly persistent to antipersistent. The results, reported in Table 3, reveal several patterns regarding the relative performance of estimators under short-run AR(1) dynamics. MSE values larger than 0.05 are shaded in gray.[9]

Because we deliberately evaluated some estimators outside their valid parameter ranges (e.g., 2ELW for $d < -0.5$), we can characterize failure modes, which can be informative for practitioners who do not know d a priori. In the absence of short-run dynamics (top panel, $\rho = 0$), the ELW estimator performs best overall, with minimal bias (-0.003) and MSE values (0.006). The 2ELW estimator has similar behavior, but fails with large bias for antipersistent processes with $d < -0.6$. This is consistent with its theoretical restriction to $d > -0.5$. The standard LW estimator also fails beyond its valid range, with bias of -1.160 and MSE of 1.358 at $d = 2.2$, in line with its known inconsistency for $d_0 > 1$ (Phillips and Shimotsu, 2004). Similarly, LWLFC shows good performance in its valid range $0 \leq d < 0.5$, extending somewhat beyond, but fails outside that range. The Velasco (V) estimator has positive bias larger than other estimators in the valid range, while the Hurvich–Chen (HC) estimator shows intermediate accuracy with generally smaller bias than V but larger MSE than the exact methods.

The addition of moderate AR(1) persistence (middle panel, $\rho = 0.5$) changes the relative

[9] This threshold is arbitrary and was chosen as a simple way to highlight obvious failures.

TABLE 3. Comprehensive Estimator Comparison

		Bias						MSE					
d	ρ	LW	V	HC	ELW	2ELW	LWLFC	LW	V	HC	ELW	2ELW	LWLFC
-2.2	0.0	1.505	0.072	0.992	-0.002	1.198	1.259	2.359	0.032	1.064	0.006	1.505	1.605
-1.8	0.0	0.991	0.057	0.548	-0.002	0.753	0.824	1.067	0.030	0.356	0.006	0.617	0.685
-1.2	0.0	0.318	0.039	0.111	-0.003	0.271	0.229	0.138	0.028	0.024	0.006	0.091	0.057
-0.6	0.0	0.020	0.031	0.025	-0.002	0.003	-0.007	0.007	0.028	0.010	0.006	0.006	0.008
-0.3	0.0	-0.002	0.024	0.011	-0.002	-0.004	-0.024	0.006	0.027	0.010	0.006	0.006	0.009
0.0	0.0	-0.007	0.026	0.005	-0.002	-0.002	-0.033	0.006	0.027	0.010	0.006	0.006	0.010
0.3	0.0	-0.006	0.024	-0.002	-0.002	-0.001	-0.046	0.006	0.027	0.010	0.006	0.006	0.014
0.6	0.0	0.003	0.029	-0.007	-0.003	0.012	-0.082	0.006	0.027	0.010	0.006	0.006	0.045
1.2	0.0	-0.125	0.036	-0.008	-0.002	-0.002	-0.125	0.022	0.028	0.010	0.006	0.006	0.024
1.8	0.0	-0.738	0.063	0.004	-0.003	-0.003	-0.733	0.560	0.031	0.009	0.006	0.006	0.557
2.2	0.0	-1.160	0.095	0.038	-0.002	-0.002	-1.156	1.358	0.036	0.011	0.006	0.006	1.353
-2.2	0.5	1.318	0.191	0.881	0.100	1.088	1.206	1.825	0.063	0.847	0.016	1.248	1.456
-1.8	0.5	0.843	0.178	0.487	0.100	0.693	0.803	0.778	0.058	0.275	0.016	0.515	0.645
-1.2	0.5	0.275	0.161	0.181	0.101	0.275	0.237	0.096	0.052	0.043	0.016	0.089	0.060
-0.6	0.5	0.110	0.150	0.132	0.100	0.100	0.099	0.019	0.050	0.027	0.016	0.016	0.017
-0.3	0.5	0.098	0.148	0.122	0.100	0.100	0.089	0.016	0.049	0.025	0.016	0.016	0.015
0.0	0.5	0.094	0.145	0.114	0.100	0.100	0.084	0.015	0.048	0.023	0.016	0.016	0.014
0.3	0.5	0.093	0.145	0.108	0.099	0.101	0.079	0.015	0.048	0.022	0.016	0.017	0.015
0.6	0.5	0.102	0.147	0.104	0.100	0.105	0.066	0.017	0.048	0.021	0.016	0.016	0.032
1.2	0.5	-0.096	0.158	0.102	0.099	0.099	-0.094	0.020	0.052	0.021	0.016	0.016	0.020
1.8	0.5	-0.735	0.183	0.114	0.100	0.100	-0.732	0.558	0.060	0.023	0.016	0.016	0.556
2.2	0.5	-1.160	0.207	0.144	0.100	0.100	-1.157	1.358	0.070	0.030	0.016	0.016	1.354
-2.2	0.8	1.250	0.536	0.925	0.414	1.111	1.205	1.638	0.316	0.905	0.179	1.278	1.454
-1.8	0.8	0.824	0.526	0.632	0.417	0.792	0.813	0.723	0.306	0.418	0.181	0.649	0.663
-1.2	0.8	0.475	0.513	0.483	0.417	0.457	0.465	0.234	0.294	0.243	0.181	0.215	0.225
-0.6	0.8	0.414	0.502	0.457	0.415	0.415	0.413	0.179	0.282	0.220	0.180	0.179	0.178
-0.3	0.8	0.409	0.499	0.450	0.416	0.416	0.408	0.174	0.279	0.214	0.180	0.180	0.174
0.0	0.8	0.406	0.503	0.446	0.416	0.419	0.406	0.172	0.282	0.211	0.180	0.184	0.172
0.3	0.8	0.406	0.499	0.441	0.417	0.419	0.405	0.172	0.279	0.206	0.181	0.183	0.172
0.6	0.8	0.396	0.501	0.437	0.417	0.417	0.390	0.164	0.280	0.202	0.181	0.181	0.171
1.2	0.8	-0.035	0.511	0.435	0.417	0.417	-0.034	0.032	0.289	0.201	0.181	0.181	0.032
1.8	0.8	-0.731	0.526	0.441	0.416	0.416	-0.728	0.558	0.304	0.205	0.181	0.180	0.556
2.2	0.8	-1.158	0.551	0.462	0.416	0.416	-1.156	1.355	0.331	0.224	0.181	0.180	1.352

Notes: Monte Carlo results for ARFIMA$(1, d, 0)$ processes with $n = 500$, $m = 56$, 10,000 replications. Shaded cells indicate MSE > 0.05.
LW = Local Whittle, V = Velasco (Kolmogorov), HC = Hurvich–Chen, ELW = Exact Local Whittle, 2ELW = Two-step ELW, LWLFC = Local Whittle robust to low-frequency contamination.

performance landscape. All estimators show upward bias, with the ELW and 2ELW methods maintaining their advantage, although with higher bias (≈ 0.100). The performance of the standard LW estimator remains good within its valid range, and actually improves somewhat for highly antipersistent cases, but still fails for extreme values of d, with bias of -0.735 at $d = 1.8$ and -1.160 at $d = 2.2$. The Velasco estimator maintains its stability but with higher mean bias for all d values. The HC estimator again shows intermediate performance, with bias increasing with $|d|$ as before.

With stronger AR(1) persistence (bottom panel, $\rho = 0.8$), the performance of all estimators suffers. Bias for central $|d|$ values exceeds 0.40 for most methods and MSE values increase by an order of magnitude. The ELW estimator has the smallest uniform bias (≈ 0.416), while the Velasco estimator exhibits bias around 0.500 for most d values. The LW estimator's behavior is somewhat erratic, with essentially the lowest bias of all estimators at $d = 1.2$ but the highest bias of all at $d = 2.2$ and $d = -2.2$. As before, the performance of 2ELW is similar to ELW for central values of d, but it fails more severely for large negative d.

In terms of overall robustness to AR(1) dynamics, the exact methods (ELW and 2ELW) show the most stability across the parameter space. Their performance degrades smoothly as autocorrelation increases. Although the behavior of the Velasco estimator is also very uniform across d values, the bias and MSE are generally higher than those of ELW and 2ELW, while the HC estimator shows intermediate robustness and more sensitivity under antipersistence. The standard LW and LWLFC estimators are most vulnerable to autocorrelation when $|d|$ is large, noting that such values are beyond their valid range. However, the exact methods' stability reflects their wider range of validity rather than robustness to short-run dynamics: within the stationary range they do not improve on the standard LW estimator, whose bias at central d is marginally smaller (e.g., at $d = 0$ with $\rho = 0.8$, 0.406 for LW against 0.416 for ELW). Among these estimators, we therefore recommend using exact local Whittle methods whenever the likely range of d is uncertain, with the exception of 2ELW when strong antipersistence is possible. Researchers may also consider the local polynomial Whittle estimator of Andrews and Sun (2004), which is designed to reduce this short-run bias at the cost of higher variance, though it is restricted to stationary processes with $|d| < 0.5$. Using a more conservative or data-driven bandwidth is another simple step towards robustness.

Additional robustness simulations reported in Appendix A indicate that this ranking is invariant to the short-run form (MA(1) and ARMA(1,1))—with the magnitude of the bias being largely driven by proximity to an autoregressive unit root—and to heavy-tailed and conditionally heteroskedastic innovations.

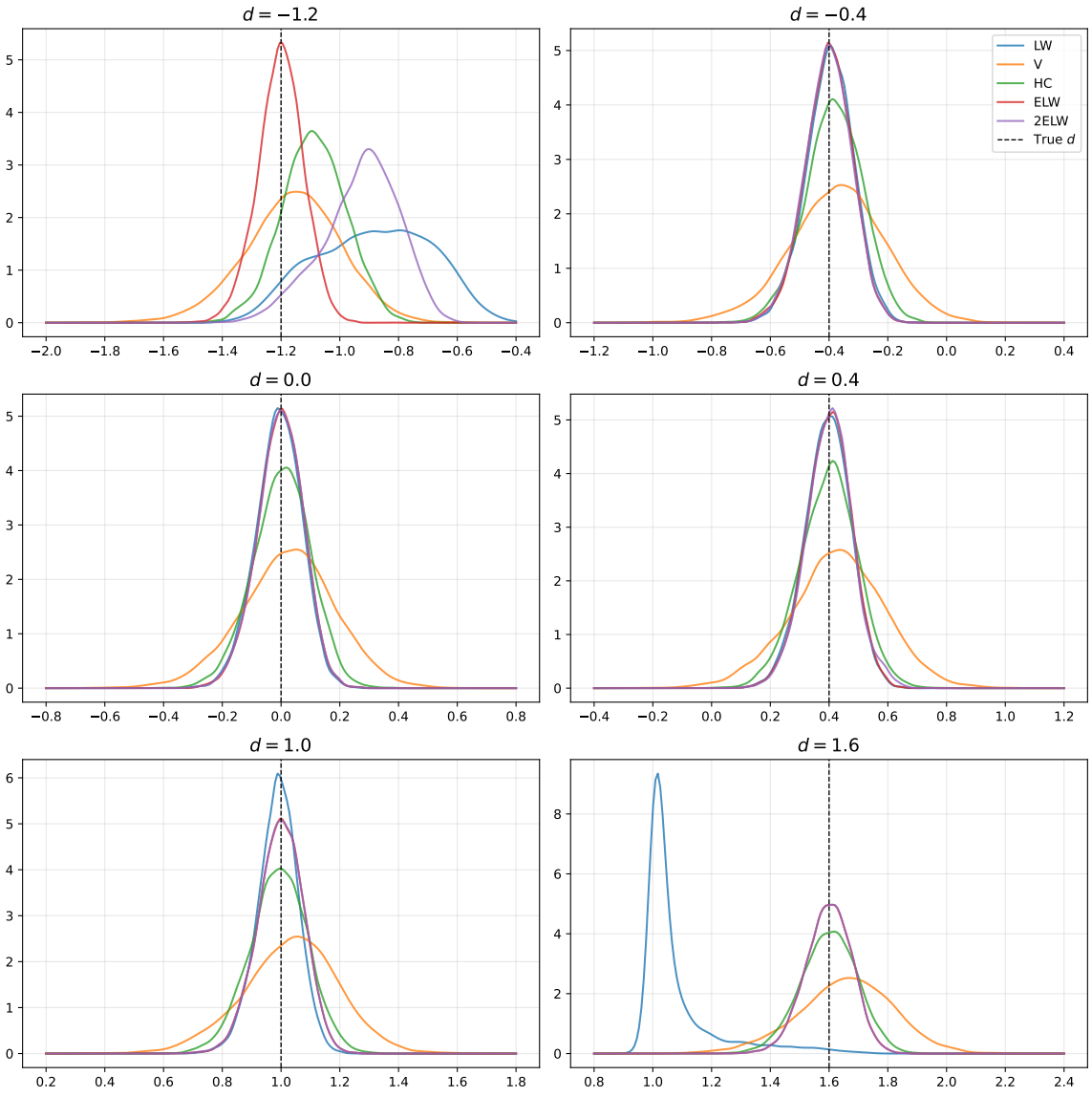

FIGURE 1. Sampling distributions of local Whittle estimators with $n = 500$ over 10,000 replications. V denotes the Velasco estimator with Kolmogorov taper.

3.2. Sampling Distribution Comparison

Figure 1 presents kernel density estimates of the sampling distributions for five estimators (LW, V, HC, ELW, and 2ELW) based on 10,000 replications of ARFIMA$(0, d, 0)$ processes with $n = 500$ observations and bandwidth $m = \lfloor n^{0.65} \rfloor$. The analysis spans six representative values of the memory parameter: $d \in \{-1.2, -0.4, 0.0, 0.4, 1.0, 1.6\}$, covering antipersistent, stationary long memory, and strongly persistent processes.

For the stationary models ($|d| < 0.5$), in accordance with theory, all estimators have

approximately symmetric distributions centered around the true parameter value. In the case of strongly nonstationary processes ($d = 1.6$), the LW estimator is inconsistent and concentrates at $d = 1.0$ (Phillips and Shimotsu, 2004, Theorem 3.2), while the exact methods (ELW and 2ELW) remain centered around the true values. For the highly antipersistent case ($d = -1.2$), in accordance with the theoretical properties, only the ELW estimator remains unbiased and concentrated around the true value. LW and 2ELW are biased upward, with means around -0.9. The V and HC estimators also have positive bias, but to a lesser degree.

3.3. Robustness to Unknown Mean

Next, we consider the sensitivity of the estimators to unknown population means. We compare performance across three approaches to mean correction: no correction ($\hat{\mu} = 0$), sample mean correction ($\hat{\mu} = \bar{X}$), and first-observation correction ($\hat{\mu} = X_1$). Table 4 shows baseline MSE values (with $\mu = 0$) and MSE ratios (with $\mu = 5$ relative to $\mu = 0$) for simulated ARFIMA$(0, d, 0)$ processes with $d \in [-2.2, 2.2]$. Ratios near unity indicate robustness to nonzero means; larger values indicate performance degradation. Since the mean is unknown a priori, for each correction we transform the data as $\tilde{X}_t = X_t - \hat{\mu}$ before applying the estimator. We apply this transformation in both cases $\mu = 0$ and $\mu = 5$. The only exception is 2ELW, which receives the original data and applies its own internal adaptive mean correction.

In the top panel, with no mean correction, the presence of a nonzero mean reveals differences in robustness. The Velasco estimator shows both good baseline performance (MSE ≈ 0.03) and robustness (MSE ratios near unity) for all d values. The LW, HC, 2ELW, and LWLFC estimators also exhibit MSE ratios near unity, but their baseline MSE values are elevated at extreme d values (e.g., LW has baseline MSE of 2.359 at $d = -2.2$), where a ratio near unity indicates consistently poor performance rather than robustness. In contrast, ELW has extremely low baseline MSE values (≈ 0.006 across d), but exhibits severe sensitivity to mean contamination for $d \leq 0.6$, especially for antipersistent processes (MSE ratio of 5.4 at $d = 0.0$, increasing to 1410 at $d = -2.2$), with robustness only for $d \geq 1.2$.

In the middle panel, we apply a sample mean correction ($\hat{\mu} = \bar{X}$). All estimators have MSE ratios near unity, meaning that their performance is similar whether the true mean is zero or nonzero. However, the sample mean correction itself (unnecessarily demeaning data with $\mu = 0$) degrades the baseline performance of ELW, with MSE of 2.099 at $d = -2.2$ and 1.120 at $d = 2.2$, while the other estimators maintain their baseline performance levels.

In the bottom panel, we consider the effects of the first-observation correction ($\hat{\mu} = X_1$). Similar to the case of the sample mean correction, all estimators have MSE ratios near unity. However, for ELW the baseline MSE effects are asymmetric: baseline MSE is elevated for $d < 0$ (4.836 at $d = -2.2$), but remains at the low level of 0.006 for $d \geq 0$.

TABLE 4. Robustness to Unknown Mean

	Baseline MSE ($\mu = 0$)						MSE Ratio ($\mu = 5$ / $\mu = 0$)					
d	LW	V	HC	ELW	2ELW	LWLFC	LW	V	HC	ELW	2ELW	LWLFC
Mean correction: None												
-2.2	2.359	0.032	1.064	0.006	1.505	1.605	0.993	0.987	0.999	1410.208	0.994	1.001
-1.8	1.077	0.029	0.355	0.006	0.618	0.684	0.993	1.024	0.988	1024.138	0.993	0.999
-1.2	0.139	0.028	0.024	0.006	0.091	0.057	0.970	1.013	0.997	537.797	0.983	0.988
-0.6	0.007	0.028	0.010	0.006	0.006	0.008	0.966	0.976	0.981	137.055	0.964	0.980
-0.3	0.006	0.027	0.010	0.006	0.006	0.009	1.010	0.993	1.004	32.781	1.004	0.985
0.0	0.006	0.027	0.010	0.006	0.006	0.010	0.978	1.006	0.977	5.359	0.979	0.970
0.3	0.006	0.027	0.010	0.006	0.006	0.014	1.016	0.985	1.020	14.515	1.016	0.997
0.6	0.007	0.028	0.010	0.006	0.006	0.047	0.973	0.963	0.981	2.369	0.974	0.936
1.2	0.022	0.027	0.010	0.006	0.006	0.025	1.007	1.009	0.997	1.019	1.006	1.014
1.8	0.557	0.031	0.009	0.006	0.006	0.554	1.006	1.003	1.011	1.032	1.027	1.006
2.2	1.359	0.036	0.011	0.006	0.006	1.355	1.001	0.993	0.990	1.015	1.010	1.001
Mean correction: $\hat{\mu} = \bar{X}$												
-2.2	2.359	0.032	1.064	2.099	1.505	1.605	0.993	0.987	0.999	0.995	0.994	1.001
-1.8	1.077	0.029	0.355	0.980	0.618	0.684	0.993	1.024	0.988	0.996	0.993	0.999
-1.2	0.139	0.028	0.024	0.121	0.091	0.057	0.970	1.013	0.997	0.977	0.983	0.987
-0.6	0.007	0.028	0.010	0.006	0.006	0.008	0.966	0.976	0.981	0.963	0.964	0.980
-0.3	0.006	0.027	0.010	0.006	0.006	0.009	1.010	0.993	1.004	1.004	1.004	0.985
0.0	0.006	0.027	0.010	0.006	0.006	0.010	0.978	1.006	0.977	0.979	0.979	0.970
0.3	0.006	0.027	0.010	0.006	0.006	0.014	1.016	0.985	1.020	1.017	1.016	0.997
0.6	0.007	0.028	0.010	0.006	0.006	0.047	0.973	0.963	0.981	0.968	0.974	0.933
1.2	0.022	0.027	0.010	0.012	0.006	0.025	1.007	1.009	0.997	1.009	1.006	1.014
1.8	0.557	0.031	0.009	0.425	0.006	0.554	1.006	1.003	1.011	1.008	1.027	1.006
2.2	1.359	0.036	0.011	1.120	0.006	1.355	1.001	0.993	0.990	1.002	1.010	1.001
Mean correction: $\hat{\mu} = X_1$												
-2.2	2.359	0.032	1.064	4.836	1.505	1.605	0.993	0.987	0.999	1.001	0.994	1.001
-1.8	1.077	0.029	0.355	3.128	0.618	0.684	0.993	1.024	0.988	1.003	0.993	0.999
-1.2	0.139	0.028	0.024	1.296	0.091	0.057	0.970	1.013	0.997	0.999	0.983	0.987
-0.6	0.007	0.028	0.010	0.278	0.006	0.008	0.966	0.976	0.981	1.003	0.964	0.980
-0.3	0.006	0.027	0.010	0.058	0.006	0.009	1.010	0.993	1.004	0.998	1.004	0.985
0.0	0.006	0.027	0.010	0.003	0.006	0.010	0.978	1.006	0.977	0.994	0.979	0.970
0.3	0.006	0.027	0.010	0.009	0.006	0.014	1.016	0.985	1.020	1.000	1.016	0.997
0.6	0.007	0.028	0.010	0.006	0.006	0.047	0.973	0.963	0.981	0.965	0.974	0.932
1.2	0.022	0.027	0.010	0.006	0.006	0.025	1.007	1.009	0.997	1.006	1.006	1.015
1.8	0.557	0.031	0.009	0.006	0.006	0.554	1.006	1.003	1.011	1.026	1.027	1.005
2.2	1.359	0.036	0.011	0.006	0.006	1.355	1.001	0.993	0.990	1.010	1.010	1.001

Notes: MSE results for ARFIMA$(0, d, 0)$ with $n = 500$, $m = 56$, 10,000 replications. Shaded cells indicate MSE > 0.05 or MSE Ratio > 2.0.
LW = Local Whittle, V = Velasco (Kolmogorov), HC = Hurvich–Chen, ELW = Exact Local Whittle, 2ELW = Two-step ELW with adaptive mean estimation applied to original series, LWLFC = Local Whittle robust to low-frequency contamination.

TABLE 5. Robustness to Time Trend

	Baseline MSE ($\beta = 0.0$)						MSE Ratio ($\beta = 0.05$ / $\beta = 0.0$)					
d	LW	V	HC	ELW	2ELW	LWLFC	LW	V	HC	ELW	2ELW	LWLFC
Trend correction: None												
-2.2	2.359	0.032	1.064	0.006	1.530	1.605	4.311	1.019	0.999	1487.482	0.995	6.333
-1.8	1.077	0.029	0.355	0.006	0.626	0.684	7.213	1.027	0.988	1099.768	0.993	11.358
-1.2	0.139	0.028	0.024	0.006	0.102	0.057	34.315	1.013	0.997	641.153	0.987	83.832
-0.6	0.007	0.028	0.010	0.006	0.007	0.008	336.676	0.976	0.981	287.097	0.973	293.749
-0.3	0.006	0.027	0.010	0.006	0.006	0.009	259.778	0.993	1.004	170.877	0.995	181.603
0.0	0.006	0.027	0.010	0.006	0.007	0.010	147.260	1.006	0.977	80.003	0.974	87.692
0.3	0.006	0.027	0.010	0.006	0.007	0.014	68.177	0.985	1.020	25.295	1.012	29.449
0.6	0.007	0.028	0.010	0.006	0.007	0.047	16.721	0.963	0.981	2.257	0.975	3.524
1.2	0.022	0.027	0.010	0.006	0.006	0.025	1.044	1.009	0.997	1.010	1.003	1.072
1.8	0.557	0.031	0.009	0.006	0.006	0.554	1.006	1.003	1.011	1.026	0.997	1.006
2.2	1.359	0.036	0.011	0.006	0.011	1.355	1.001	0.993	0.990	1.010	0.998	1.001
Trend correction: linear OLS detrending												
-2.2	2.551	0.032	1.064	2.443	1.530	1.585	0.994	0.987	0.999	0.994	0.995	1.001
-1.8	1.211	0.029	0.355	1.174	0.626	0.677	0.994	1.024	0.988	0.994	0.993	1.000
-1.2	0.180	0.028	0.024	0.177	0.102	0.054	0.973	1.013	0.997	0.974	0.987	0.988
-0.6	0.008	0.028	0.010	0.007	0.007	0.009	0.977	0.976	0.981	0.973	0.973	0.990
-0.3	0.006	0.027	0.010	0.006	0.006	0.009	1.001	0.993	1.004	0.995	0.995	0.985
0.0	0.007	0.027	0.010	0.007	0.007	0.010	0.974	1.006	0.977	0.974	0.974	0.969
0.3	0.007	0.027	0.010	0.007	0.007	0.013	1.012	0.985	1.020	1.012	1.012	0.987
0.6	0.008	0.028	0.010	0.007	0.007	0.029	0.974	0.963	0.981	0.978	0.975	0.952
1.2	0.015	0.027	0.010	0.009	0.006	0.020	0.989	1.009	0.997	0.980	1.003	1.043
1.8	0.317	0.031	0.009	0.317	0.006	0.308	1.012	1.003	1.011	1.013	0.997	1.013
2.2	0.870	0.036	0.011	1.029	0.011	0.837	1.011	0.993	0.990	1.006	0.998	1.009

Notes: MSE results for ARFIMA$(0, d, 0)$, $n = 500$, $m = 56$, 10,000 replications. Shaded cells indicate MSE > 0.05 or MSE Ratio > 2.0.
LW = Local Whittle, V = Velasco (Kolmogorov), HC = Hurvich–Chen, ELW = Exact Local Whittle, 2ELW = Two-step ELW with linear detrending and adaptive mean estimation applied to original series, LWLFC = Local Whittle robust to low-frequency contamination.

Overall, these results demonstrate that the Velasco-tapered LW estimator provides remarkable robustness to unknown means, corrected or not, over the full range of d values. LW, HC, and 2ELW are largely unaffected, but have ranges of d values where they perform much worse than Velasco. For ELW, the best mean correction critically depends on the expected range of d, which is precisely the intuition behind the 2ELW estimator's adaptive mean correction.

3.4. Robustness to Linear Time Trends

The Monte Carlo results in Table 5 examine the sensitivity of the estimators to linear deterministic time trends across the parameter range. The experiment involves simulated ARFIMA$(0, d, 0)$ processes under two scenarios: no trend ($\beta = 0.0$) and linear trend ($\beta = 0.05$). For both specifications, we report the performance both with and without

detrending. As in the previous section, this table displays baseline MSE values (for $\beta = 0.0$) and MSE ratios ($\beta = 0.05$ relative to $\beta = 0.0$). For LW, V, HC, and ELW, in the "linear OLS detrending" panel we apply the estimators to preprocessed data that have been detrended (i.e., residuals from an OLS regression on a constant and t). In contrast, we always apply 2ELW to the original unprocessed data and allow it to apply its own internal linear detrending. As a result, the 2ELW results are identical in the top and bottom panels.

With no trend correction (top panel), the Velasco- and Hurvich–Chen-tapered LW estimators demonstrate both good baseline MSE within their valid range and robustness to a linear trend (i.e., MSE ratios are near unity). In contrast, LW, ELW, and LWLFC are highly sensitive to the trend for $d \leq 0.6$: MSE ratios for LW exceed 100 for $-0.6 \leq d \leq 0.0$, and those for ELW climb as d falls, reaching 1487 at $d = -2.2$. The baseline MSE of 2ELW is elevated for $d \leq -1.2$, yet it shows good robustness to the trend with MSE ratios near unity for all d values.

Detrending by OLS (bottom panel) equalizes performance between trend scenarios, with all estimators exhibiting MSE ratios near unity. However, like demeaning, detrending when no trend is actually present can be detrimental to baseline performance for ELW in particular: baseline MSE increases from 0.006 to 2.443 at $d = -2.2$ and 1.029 at $d = 2.2$.

These results illustrate an important practical point: the Velasco- and Hurvich–Chen-tapered LW estimators provide robustness to linear deterministic trends without any preprocessing. The internal trend correction of 2ELW is also effective. On the other hand, the LW, ELW, and LWLFC estimators fail unless the researcher detrends the data, and may still fail in spite of the correction for more extreme values of d.

4. Empirical Applications

We now turn from controlled Monte Carlo experiments to real economic data, where the memory parameter is unknown and the data may violate ideal assumptions. This section replicates and extends the empirical analysis of Hurvich and Chen (2000). Using their original datasets, but now comparing across multiple estimators, we examine anomalous estimates, bandwidth selection, and structural breaks. Our emphasis is methodological: each series illustrates how the estimators behave on real data and how to approach model specification and estimator choice, with lessons that extend beyond the particular series examined.

4.1. Replication and Extension of Table III

We begin by replicating and extending the empirical analysis in Table III of Hurvich and Chen (2000), who applied their complex tapered LW estimator to seven datasets including

TABLE 6. Hurvich and Chen (2000) Datasets: LW Estimator Comparison

			Original	Replication				
Series	n	m	HC	LW	V	HC	ELW	2ELW
Global temp.	1632	130	0.45	0.50	0.44	0.45	0.50	0.47
			(0.060)	(0.044)	(0.076)	(0.060)	(0.044)	(0.044)
S&P 500	8432	1383	0.99	0.98	0.98	0.97	0.99	0.98
			(0.018)	(0.013)	(0.023)	(0.017)	(0.013)	(0.013)
Inflation, US	491	40	0.57	0.63	0.66	0.56	0.64	0.64
			(0.123)	(0.079)	(0.137)	(0.121)	(0.079)	(0.079)
Inflation, UK	491	40	0.33	0.46	0.49	0.34	0.47	0.47
			(0.123)	(0.079)	(0.137)	(0.121)	(0.079)	(0.079)
Inflation, FR	491	40	0.67	0.46	0.82	0.68	0.50	0.45
			(0.123)	(0.079)	(0.137)	(0.121)	(0.079)	(0.079)
Real wages, US	492	35	1.43	1.06	1.56	1.43	0.06	1.29
			(0.121)	(0.085)	(0.147)	(0.132)	(0.085)	(0.085)
Ind. prod., US	492	100	1.34	1.00	1.31	1.36	0.10	1.31
			(0.075)	(0.050)	(0.087)	(0.071)	(0.050)	(0.050)

Notes: Estimates of d with asymptotic standard errors in parentheses. The Original column shows results from Hurvich and Chen (2000) Table III for HC. Replication columns report results from multiple estimators: LW = Local Whittle, V = Velasco (Kolmogorov), HC = Hurvich–Chen, ELW = Exact Local Whittle, 2ELW = Two-step ELW. The replication HC column reports standard errors based on their variance approximation (rather than asymptotic standard errors) for direct comparison with the original.

economic, financial, and environmental time series. Motivated by their work, in Table 6 we compare five LW estimators using the same datasets.[10]

The global temperature series contains seasonally adjusted monthly temperatures for the northern hemisphere from 1854–1989, computed as deviations from monthly averages relative to 1950–1979 (Beran, 1994). The S&P 500 series consists of the natural logarithms of the daily stock index levels from July 1962 to December 1995. The remaining series were drawn from the International Monetary Fund's International Financial Statistics database and consist of monthly economic indicators from January 1957 to December 1997. These include CPI-based inflation rates for the U.S., U.K., and France (differences in logarithms of CPI), the logarithm of U.S. real manufacturing wages,[11] and the logarithm of U.S. industrial production. All of these economic series were seasonally adjusted. We intentionally maintain the original sample periods to permit direct comparison with the published estimates. In Section 4.4, we analyze in detail the French inflation data, extended through 2025.

Table 6 compares the original Hurvich and Chen (2000) results (for the HC estimator) with our independent implementations of all five estimators. For all estimators, we use the

[10]The reported number of observations is increased by one because Hurvich and Chen (2000) report the number of observations after first differencing.

[11]We note one important exception in our replication. Since the original IMF data on U.S. real manufacturing wages no longer appear to be available, we instead use FRED average hourly earnings of production and nonsupervisory employees in manufacturing (CES3000000008) divided by CPI, which matches the published HC estimate.

same number of frequencies m as in the original study, where bandwidths were selected based on visual inspection of log-log periodogram plots. For the HC-tapered LW estimator, the agreement between our results and the original estimates is close for all datasets, with differences typically at the second decimal place or smaller.

In terms of the economic implications of these estimates, there is broad agreement across estimators. Global temperatures, with $\hat{d} \in [0.44, 0.50]$, appear to be stationary with moderate long memory. The S&P 500 index appears to have near-unit-root behavior, with $\hat{d} \in [0.97, 0.99]$. The inflation series reveal heterogeneous persistence across countries: U.S. inflation has moderate persistence, with $\hat{d} \in [0.56, 0.66]$, while U.K. inflation has somewhat weaker dependence, with $\hat{d} \in [0.34, 0.49]$. The five estimators yield widely varying estimates of inflation persistence in France, with $\hat{d} \in [0.45, 0.82]$. Because this range includes the nonstationarity boundary at 0.5, the estimators disagree on whether the series is even stationary, a case we examine in detail in Section 4.4.

U.S. real manufacturing wages appear to be nonstationary, with $\hat{d} \in [1.06, 1.56]$ (with the notable exception of ELW), suggesting that wage shocks have permanent effects. The lower estimate from LW ($\hat{d} = 1.06$) is in line with the known inconsistency of LW for $d > 1$. ELW's extremely low estimate ($\hat{d} = 0.06$) reflects sensitivity to the unknown mean relative to 2ELW and other methods based on tapering. We will return to this point in the following section. Similarly, industrial production shows evidence of nonstationarity, with estimates $\hat{d} \in [1.00, 1.36]$ (again excluding ELW, and with LW being apparently bounded near unity), indicating that productivity shocks have persistent effects on growth. Overall, these results add nuance to the traditional $I(0)$ or $I(1)$ classifications of time series, underscoring the empirical relevance of fractional integration.

4.2. Anomalous Memory Estimate for U.S. Industrial Production

We now return to the U.S. industrial production time series, where ELW yields a spuriously low estimate ($\hat{d} = 0.10$), while the tapered estimators and 2ELW cluster in $\hat{d} \in [1.31, 1.36]$. Even the inconsistent untapered LW estimator ($\hat{d} = 1.00$) yields a more reasonable estimate than ELW. To understand this difference, we plot the objective functions for each estimator in Figure 2. The LW-based objective functions (LW, V, HC) are all convex with a single global minimum. The ELW objective, on the other hand, is non-convex and has two local minima: a spurious global minimum at $\hat{d} = 0.10$ and a shallower minimum near $d = 1$. When we apply the ELW estimator to demeaned data, an estimator discussed in Section 3 of Shimotsu (2010) (denoted ELW-DM in the figure), the spurious minimum is removed and we obtain the estimate $\hat{d} = 1.08$. This suggests that the low estimate produced by ELW is due to the fact that it assumes the mean is known and equal to zero.

The 2ELW estimator confronts the unknown mean by applying the piecewise adaptive

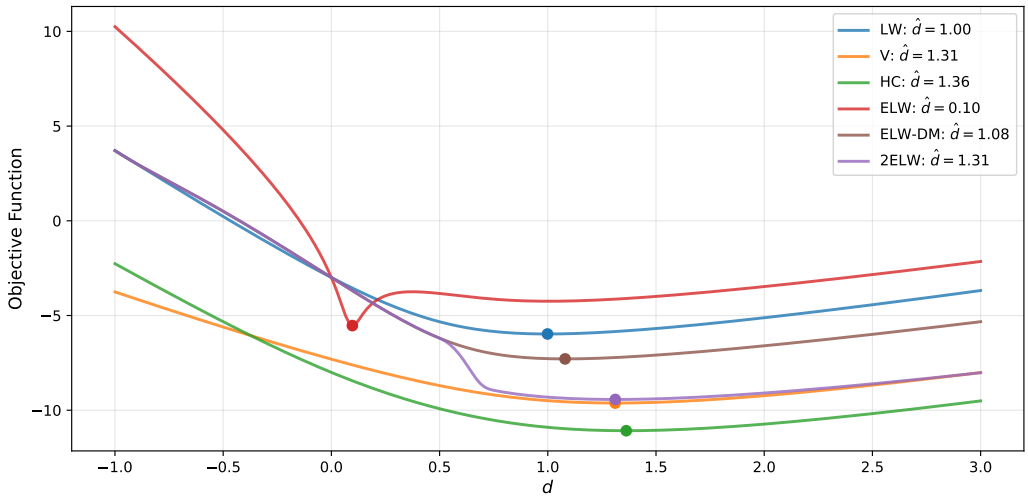

FIGURE 2. Local Whittle objective functions for U.S. industrial production (log monthly index, 1957–1997). The LW-based estimators (LW, V, HC) have convex objective functions. The ELW objective is non-convex with two local minima, its global minimum falling at the spurious value $\hat{d} = 0.10$. The 2ELW and ELW-DM objectives coincide for $d \leq 1/2$, and 2ELW's adaptive mean correction yields a single minimum at $\hat{d} = 1.31$.

weight function defined in (6). Because $w(d) = 1$ for $d \leq 0.5$, the ELW-DM and 2ELW objective functions coincide exactly up to $d = 0.5$. After $d = 0.5$, the weight function begins to apply positive weight to $\hat{\mu} = X_1$, causing the 2ELW objective function to diverge from that of ELW-DM. Because $w(d)$ is continuously differentiable, the transition is smooth rather than kinked. The weight shifts fully from $\hat{\mu} = \bar{X}$ to $\hat{\mu} = X_1$ by $d = 0.75$, beyond which the function flattens and attains a single global minimum at $\hat{d} = 1.31$.

Although a gap between the ELW estimate and the mean-robust estimates flags possible mean contamination, the absence of such a gap (agreement across estimators) does not imply the absence of contamination. Short-run dynamics, for example, can bias all estimators together (Section 3.1).

4.3. Bandwidth Selection for Daily Values of the S&P 500 Index

We now consider the effects of bandwidth choice m. In applied work it is common to choose $m = \lfloor n^{\alpha} \rfloor$ with α ranging from roughly 0.5 to 0.8. Monte Carlo and empirical work in the literature often uses the rule $m = \lfloor n^{0.65} \rfloor$ as a baseline. This rate was used by Shimotsu and Phillips (2005) and Shimotsu (2010) in their simulations and implemented as the default in both Stata's `whittle` command (Baum et al., 2020) and PyELW (Blevins, 2026). In empirical examples, Shimotsu (2010) used the slightly less conservative $m = \lfloor n^{0.7} \rfloor$.

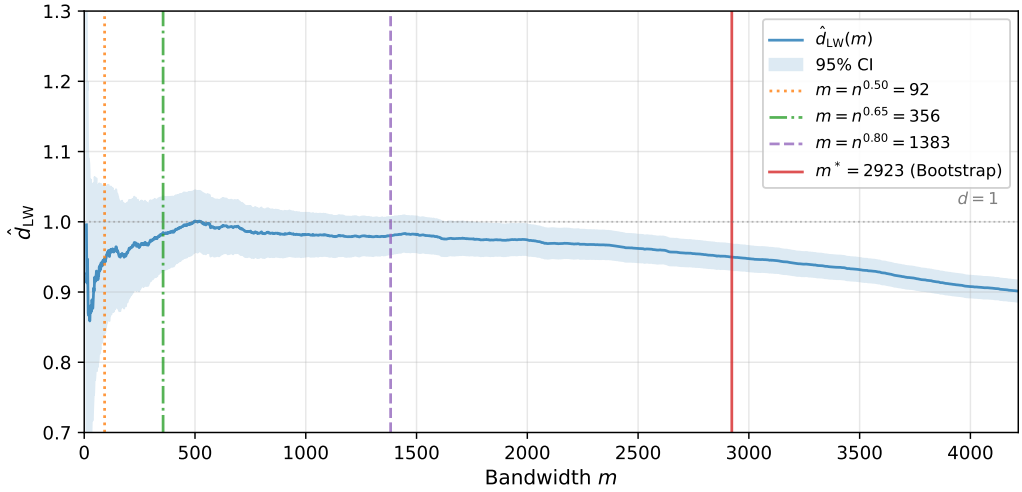

FIGURE 3. Local Whittle estimates by bandwidth using S&P 500 data. The plotted line shows estimates $\hat{d}_{\mathrm{LW}}(m)$ with pointwise variance-based bands $\pm 1.96/(2\sqrt{m})$. Vertical lines indicate bandwidth choices: the power rules $m = n^{0.5}$ (dotted), $m = n^{0.65}$ (dash-dotted), and $m = n^{0.8}$ (dashed), and the Arteche and Orbe (2017) optimal m^* (solid).

Baillie et al. (2014) proposed cross-validation approaches focused on forecasting performance, while Arteche and Orbe (2017) developed a bandwidth selection method based on minimizing a bootstrap approximation of the mean squared error. Specifically, an initial LW estimate $\hat{d}$ is used to form the standardized periodogram $I_X(\lambda_j)\lambda_j^{2\hat{d}}$, removing the power-law component implied by the memory parameter. This standardized periodogram is locally resampled to generate bootstrap samples, and for each candidate bandwidth m the LW estimator is recomputed to approximate its MSE. The optimal bandwidth m^* minimizes this bootstrap MSE.

We now illustrate the effects of bandwidth selection using the daily S&P 500 index series ($n = 8{,}432$) as an example. Figure 3 plots the LW estimates $\hat{d}_{\mathrm{LW}}(m)$ as a function of bandwidth m, from $m = 10$ to $m = n/2$. The shaded region shows pointwise 95% confidence bands $\hat{d}_{\mathrm{LW}}(m) \pm 1.96/(2\sqrt{m})$. Estimates range from approximately 0.86 at extreme values of m to a peak of approximately 1.0 near $m = 500$. The confidence intervals narrow as m increases, reflecting the variance reduction from using additional frequencies.

The vertical lines in Figure 3 indicate different bandwidth choices. Power rules ($m = n^{0.5}$ through $m = n^{0.8}$) result in bandwidth choices from $m = 92$ to $m = 1{,}383$,[12] which yields estimates $\hat{d}_{\mathrm{LW}} \in [0.948, 0.984]$. Table 7 compares the estimates for different bandwidth selection methods. The 95% confidence intervals from the power rule methods each contain

[12]To match Hurvich and Chen (2000), we use $m = \mathrm{round}(n^\alpha)$ here rather than $m = \lfloor n^\alpha \rfloor$, which is used elsewhere in this paper.

TABLE 7. S&P 500: Bandwidth Selection Comparison

Method	Rule	m	$\hat{d}_{\text{LW}}$	SE	95% CI
Power Rule	$m = n^{0.50}$	92	0.948	0.052	$(0.846, 1.050)$
	$m = n^{0.65}$	356	0.984	0.026	$(0.932, 1.036)$
	$m = n^{0.80}$	1,383	0.980	0.013	$(0.954, 1.006)$
Arteche and Orbe (2017)	Min. Bootstrap MSE	2,923	0.950	0.009	$(0.931, 0.968)$

Notes: Logarithm of S&P 500 daily stock index value, $n = 8{,}432$. Hurvich and Chen (2000) used $m = n^{0.80}$. Asymptotic standard errors reported with 95% confidence intervals. Bootstrap MSE bandwidth selected by minimizing bootstrap MSE with $B = 200$ replications and resampling width $k_n = 255$ following Arteche and Orbe (2017).

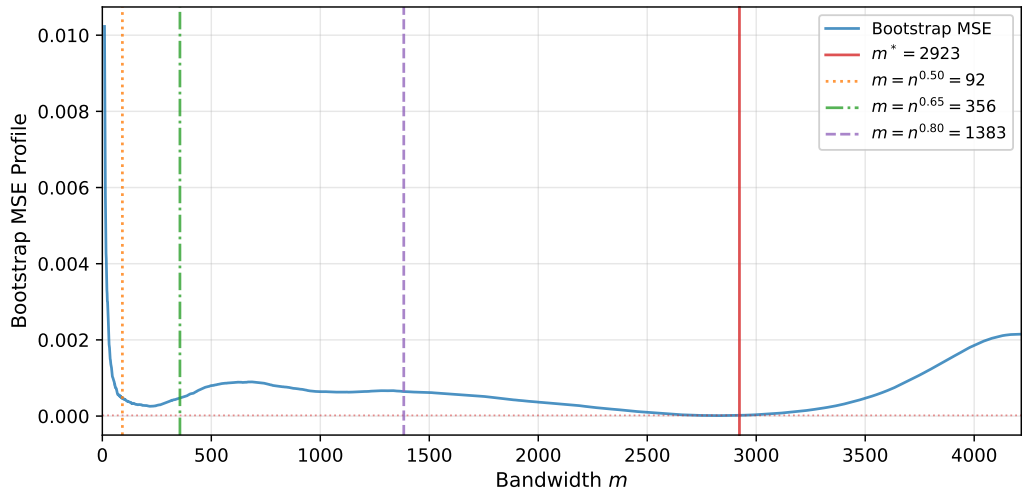

FIGURE 4. Bootstrap MSE profile for S&P 500 data. The blue line represents the estimated MSE for each bandwidth, with the minimum at $m^* = 2{,}923$ indicated by the red vertical line. Power rule bandwidths are indicated by vertical lines with the same styles as in Figure 3.

$d = 1.0$, consistent with a unit-root process.

We also apply the bootstrap MSE minimization procedure of Arteche and Orbe (2017), which selects $m^* = 2{,}923$ and yields $\hat{d}_{\text{LW}} = 0.950$. We note that this bandwidth is much larger than that of any of the power rules, which imply conservative choices for this relatively large sample. This occurs due to the relatively weak short-run dynamics: the resulting locally standardized periodogram is relatively flat, leading to a large bandwidth choice m^*. The bootstrap MSE profile, displayed in Figure 4, shows the bias-variance trade-off. MSE is high at small m due to high variance, then decreases to a minimum at $m^* = 2{,}923$ before rising again as m approaches $n/2$, where the bias begins to dominate. Across bandwidths, the estimates are consistent with d at or just below unity.

4.4. Structural Breaks and Long Memory in French Inflation

The wide range of French inflation estimates in Table 6, where $\hat{d} \in [0.45, 0.82]$, raises the question: which estimator should practitioners trust? Disagreement of this magnitude, with estimates on both sides of the nonstationarity boundary $d = 0.5$, has implications for inference, forecasting, and policy. One concern is that structural breaks may inflate long-memory estimates:[13] Diebold and Inoue (2001) and Granger and Hyung (2004) showed that regime-switching and occasional mean shifts mimic the low-frequency behavior of fractional integration, yielding spuriously positive estimates of d.

A natural approach is to split the sample at break points: within a stable regime the mean is constant, so within-regime estimates are free of shift-induced upward bias.[14] This yields a useful check: genuine long memory should remain present in every regime, whereas spurious memory that is an artifact of level shifts should appear weaker within regimes (Shimotsu, 2006).

Because a structural break analysis is more informative over a long period, we use an extended French CPI series from January 1955 to March 2025 (longer than the 1957–1997 window used by Hurvich and Chen (2000)), yielding $n = 842$ monthly inflation observations.[15] We apply the structural break detection procedure of Bai and Perron (1998, 2003).[16] Minimizing the BIC over the full sample selects five breaks, but that partition results in three segments of only two to three years, too short for reliable semiparametric estimation. We therefore focus on the two most prominent breaks, which also correspond with important economic events: March 1973 (before the first oil shock) and October 1984 (coinciding with the mid-1980s disinflation). Figure 5 displays the annualized inflation rates along with the detected break dates and regime-specific means and standard deviations.

In Table 8, we report the memory parameter estimates for French inflation using six local Whittle estimators. The top panel reports estimates for the extended 1955–2025 sample, including the LWLFC estimator of Hou and Perron (2014). For comparability with the original analysis and with our replication in Table 6, we retain the bandwidth $m = 40$ chosen by Hurvich and Chen (2000). On the extended sample this corresponds to the power rule $m = \lfloor n^{0.55} \rfloor$. Across the six estimators, full-sample estimates now span

[13] Indeed, Caporale, Gil-Alana, and Poza (2022) documented multiple structural breaks in G7 inflation series over 1973–2020.

[14] Within-regime estimates remain sensitive to the regime mean itself, which is a concern for ELW in particular (Section 3.3).

[15] The series is the consumer price index for France (all items) from the OECD Main Economic Indicators, retrieved from FRED (series `FRACPIALLMINMEI`). Over 1957–1997 it coincides exactly with the series used by Hurvich and Chen (2000), which was drawn from the International Monetary Fund's International Financial Statistics database.

[16] Conventional break tests are not robust to long memory and may over-detect breaks in its presence. Iacone, Leybourne, and Taylor (2013, 2014) develop break tests designed to remain valid under fractional integration.

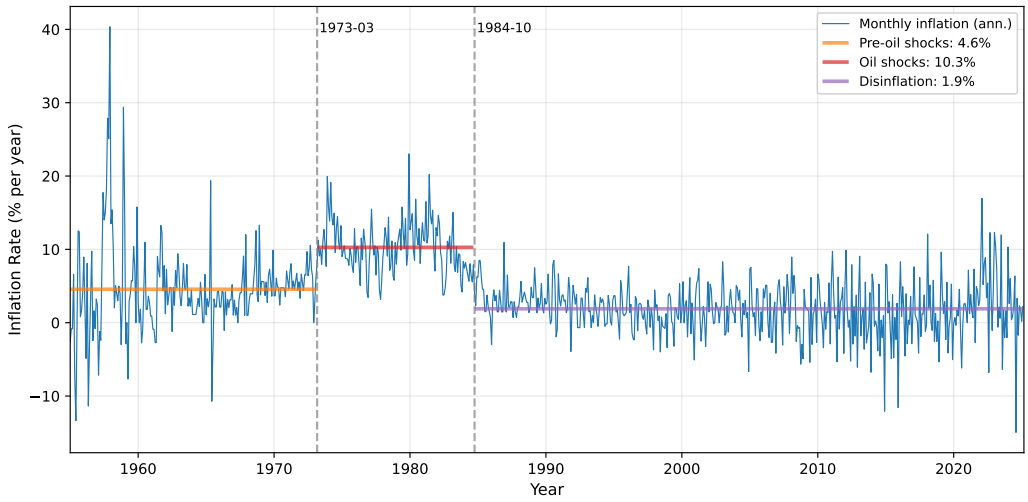

FIGURE 5. French inflation (annualized differences in log monthly CPI) with structural breaks. Horizontal lines indicate regime means: 4.6%/yr (pre-1973), 10.3%/yr (1973–1984), and 1.9%/yr (post-1984); within-regime standard deviations are 6.0%, 3.5%, and 3.6%. Break dates detected using Bai and Perron (2003) methodology.

$\hat{d} \in [0.121, 0.801]$. LWLFC yields the lowest estimate among all estimators, with $\hat{d} = 0.121$, and the corresponding 95% confidence interval contains zero. This suggests that level shifts are contributing to the low-frequency power, which the other estimators attribute to memory.

To investigate this further, in Panels A and B of Table 8, we report the memory parameter estimates for each of these regimes with two bandwidth selection approaches. Panel A applies the same implied power rule from the full sample ($m = \lfloor n^{0.55} \rfloor$), yielding small subsample bandwidths of $m \in \{19, 15, 30\}$. Panel B uses the bootstrap-MSE-optimal selection procedure of Arteche and Orbe (2017), which results in larger subsample bandwidths of $m \in \{97, 30, 31\}$. We note that in all panels of this table, for 2ELW we specify a trend of order zero (i.e., demeaning only).

The full-sample LW and tapered LW estimates (V and HC) consistently exceed the subsample estimates. This is the pattern level shifts induce in estimators that do not account for a changing mean. However, the size of the gap differs across estimators. It is largest for the tapered estimators: in Panel B, the full-sample HC estimate (0.711) exceeds the subsample estimates by 0.324–0.433, and the Velasco gaps are larger still. Tapering provides robustness to polynomial trends and nonstationarity, but not level shifts. The Velasco subsample estimates are near zero in both panels, but the order-three taper discards two-thirds of the periodogram ordinates, and we therefore treat these estimates as unreliable at subsample bandwidths rather than as evidence against within-regime memory.[17] For the

[17] Given the Panel A bandwidths $m \in \{19, 15, 30\}$, the order-three Kolmogorov taper retains only 6, 5, and

TABLE 8. Inflation in France: Subsample Analysis with Detected Structural Breaks

Period	n	m	LW	V	HC	ELW	2ELW	LWLFC
Full sample	842	40	0.495	0.801	0.711	0.518	0.492	0.121
			(0.079)	(0.137)	(0.097)	(0.079)	(0.079)	(0.079)
Panel A: Power rule bandwidth ($m = n^{0.55}$)								
Pre-oil shocks	218	19	0.070	0.087	0.139	0.127	0.090	0.070
			(0.115)	(0.199)	(0.140)	(0.115)	(0.115)	(0.115)
Oil shocks	139	15	0.402	−0.104	0.376	−0.009	0.423	0.402
			(0.129)	(0.224)	(0.158)	(0.129)	(0.129)	(0.129)
Disinflation	485	30	0.350	0.020	0.255	0.360	0.368	0.295
			(0.091)	(0.158)	(0.112)	(0.091)	(0.091)	(0.091)
Panel B: Bootstrap-MSE-optimal bandwidth m^*								
Pre-oil shocks	218	97	0.340	0.155	0.341	0.477	0.479	0.340
			(0.051)	(0.088)	(0.062)	(0.051)	(0.051)	(0.051)
Oil shocks	139	30	0.409	0.071	0.387	0.572	0.445	0.409
			(0.091)	(0.158)	(0.112)	(0.091)	(0.091)	(0.091)
Disinflation	485	31	0.348	0.076	0.278	0.360	0.366	0.293
			(0.090)	(0.156)	(0.110)	(0.090)	(0.090)	(0.090)

Notes: Estimates of d with asymptotic standard errors in parentheses. French inflation is monthly log-differenced CPI from January 1955 to March 2025. Structural breaks detected following Bai and Perron (2003): March 1973, October 1984. Mean inflation: 4.6%/yr (pre-1973), 10.3%/yr (1973–1984), 1.9%/yr (post-1984). Panel A uses the same power rule as the full sample. Panel B uses bootstrap MSE-optimal bandwidth selection (Arteche and Orbe, 2017).

Velasco estimator, the evidence that the level shifts inflate the estimate comes instead from the full-sample estimate, the largest among the six and well above the mean-robust 2ELW value of 0.492. For the untapered LW estimator the gap is smaller: the full-sample value (0.495) exceeds the subsample estimates (0.340, 0.409, and 0.348 in Panel B) by 0.086–0.155. The ELW estimate of −0.009 for the oil-shocks regime (Panel A) reflects a different failure mode: sensitivity to the regime mean rather than the level shifts themselves.

In Panel B, the mean-robust 2ELW estimator yields 0.479, 0.445, and 0.366 across the three regimes, close to its full-sample value and well above zero. Excluding Velasco, the other five estimators provide a similar assessment: they agree to within 0.088–0.185 inside each regime in Panel B, and all fifteen of the corresponding 95% confidence intervals exclude zero. This includes the level-shift-robust LWLFC estimator, with $\hat{d} \in [0.293, 0.409]$ within the regimes, where no level shifts remain. Its low full-sample estimate thus reflects the shifts, not an absence of memory. Since the estimates remain near 0.4 across subsamples rather

10 periodogram ordinates respectively. The Panel B bandwidths $m \in \{97, 30, 31\}$ leave 32, 10, and 10.

than collapsing toward zero, this suggests the long memory is genuine rather than spurious.

The pre-oil-shocks regime illustrates how sensitive subsample estimates can be to the bandwidth. We examine this using LW, the estimator for which the bootstrap-MSE procedure of Arteche and Orbe (2017) is designed. Under the conservative power rule (Panel A, $m = 19$), the LW estimate for this regime is 0.070, with a 95% confidence interval that contains zero. The MSE-optimal bandwidth is much larger ($m = 97$), and there the estimate is 0.340, with a confidence interval that excludes zero. The apparent absence of memory in this regime is thus specific to the small bandwidth,[18] and moderate persistence in line with the other two regimes is indicated by larger bandwidths.

Formal tests for spurious long memory (Shimotsu, 2006; Ohanissian, Russell, and Tsay, 2008; Qu, 2011) test the null of genuine, constant-memory fractional integration against shift- or trend-contaminated short memory. For a series in which the two coexist, a rejection signals the presence of the shifts, not the absence of genuine memory (Qu, 2011, Corollary 1). This is precisely the pattern we find: the Qu (2011) test rejects the null on the full sample ($W = 1.30$, significant at the 5% level) but does not reject in any of the three regimes ($W = 0.65$, 0.64, and 0.99, all below the 10% critical value of 1.02), consistent with level shifts contaminating the full sample and genuine memory remaining once the regimes are isolated (though non-rejection on short subsamples is weak evidence).[19]

Because long memory and level shifts both concentrate power at low frequencies, it is difficult to separate them. We draw two conclusions from the subsample analysis. First, the regime level shifts appear to be real and to coexist with long memory. They nonetheless inflate the mean-sensitive estimators—the tapered ones most severely—and pull the LWLFC estimate down to 0.121. Second, the evidence is most consistent with genuine long memory of roughly 0.4: the mean-robust 2ELW estimate is stable across the regimes, close to its full-sample value, and does not collapse on subsamples. Therefore, the answer to the opening question is not a single estimator, but rather the comparison exercise that reveals the level shifts and the memory that survives them.

5. Guidance for Practitioners

This section distills the preceding theoretical, Monte Carlo, and empirical sections to provide practical recommendations for selecting and implementing local Whittle estimators in applied work. Under ideal conditions, every estimator behaves as theory predicts; the difficulty is

[18] Starting from the baseline rule $m = \lfloor n^{0.65} \rfloor = 33$, the LW estimate remains between 0.31 and 0.38, with confidence intervals excluding zero, at every bandwidth from 33 to 97.

[19] Following Qu (2011), we use $m = \lceil n^{0.70} \rceil$ and trimming $\varepsilon = 0.05$, which is recommended for samples with $n < 500$, as in our subsamples. This yields $m = 112$ for the full sample and $m \in \{44, 32, 76\}$ for the regimes. The optional ARFIMA-AIC prewhitening procedure leaves the statistics unchanged, which our replication materials confirm using the original R code).

TABLE 9. Summary of Local Whittle Estimator Properties

Estimator	Valid range of d	Asymptotic variance	Unknown mean	Time trend	Level shifts
LW	$(-1/2, 3/4)$[a]	$1/4$	robust	sensitive	sensitive
V	$(-1/2, 5/2)$[b]	$3.01/4$	robust	robust	sensitive
HC	$(-1/2, 3/2)$	$1.5/4$	robust	robust	sensitive
ELW	$(-\infty, \infty)$[c]	$1/4$	sensitive	sensitive	sensitive
2ELW	$(-1/2, 2)$[d]	$1/4$	robust	robust	sensitive
LWLFC	$[0, 1/2)$	$1/4$	robust	sensitive	robust

Notes: "robust" denotes consistency without preprocessing while "sensitive" denotes material bias unless the component is absent or removed.

[a] Consistent for $d \in (-1/2, 1)$ and asymptotically normal for $d \in (-1/2, 3/4)$ (Velasco, 1999).

[b] Kolmogorov taper ($p = 3$), used in our cross-method comparisons and empirical applications.

[c] Valid for all d provided the optimization interval has width at most $9/2$.

[d] Range $(-1/2, 2)$ with mean correction, narrowing to $(-1/2, 7/4)$ with detrending.

that no single one dominates across the scenarios we considered, so practitioners must match their choice to the features of their data.

Table 9 summarizes the properties that drive this choice. It displays each estimator's range of validity, its asymptotic variance, and its robustness to an unknown mean, a deterministic trend, and low-frequency level shifts.

5.1. Expected Parameter Range

The first consideration for choosing an estimator should be the expected parameter range. If the researcher expects that the process is stationary, the standard LW and ELW estimators attain the minimal asymptotic variance of $1/4$. For applications where low-frequency contamination from level shifts is suspected, the LWLFC estimator provides robustness without loss of efficiency, but it is restricted to stationary processes with $d \in [0, 1/2)$. For series where d could lie outside the stationary and invertible range, practitioners should consider using the ELW and 2ELW estimators. Tapered LW estimators offer an intermediate solution. They extend the range of valid parameter values compared to LW, but at the cost of higher variance.

The choice is more difficult for antipersistent processes. ELW maintains consistency even for strongly antipersistent processes in ideal settings, and the Velasco estimator remains accurate in our simulations well below $d = -1/2$, outside its valid range. However, the antipersistent region is precisely where ELW is extremely sensitive to unknown deterministic components, and the 2ELW estimator fails entirely for $d < -0.6$ in our simulations. When the researcher suspects a process is antipersistent, we suggest comparing the ELW and

Velasco estimates. If they agree, it suggests genuine antipersistence. However, if ELW produces substantially higher estimates than Velasco, this may indicate contamination from unknown deterministic components.[20]

5.2. Robustness Considerations

Short-run dynamics affect all local Whittle estimators considered, inducing a positive bias that grows with the proximity of the autoregressive root to unity (Section 3.1 and Appendix A). Practitioners who suspect non-trivial short-run dynamics should expect all estimates to be shifted upward and prefer the exact estimators ELW and 2ELW for their wider range of validity (though 2ELW should be avoided when strong antipersistence is suspected). More conservative bandwidth choices (i.e., smaller values of m) can help mitigate contamination from short-run dynamics affecting higher frequencies (Henry and Robinson, 1996; Henry, 2001).

We saw that the ELW estimator is highly sensitive to nonzero means and linear trends, particularly for antipersistent processes (Sections 3.3–3.4). When analyzing data with potential nonzero means or trends, practitioners should consider using the 2ELW estimator, noting that its range is restricted to $d \in (-1/2, 7/4)$ when detrending. However, we caution that demeaning or detrending when it is not necessary can also be detrimental, especially for ELW when $|d|$ is large.

Overall, the tapered estimators and 2ELW are robust to deterministic components and valid across a wide range of memory parameters, which makes them the safer default when the properties of the data are uncertain. Because LWLFC is valid only within the stationary range, and the guarantees for LW extend only slightly beyond it, both are best reserved for series likely to be stationary. And because ELW is sensitive to deterministic components, it should be applied to demeaned data or replaced by the 2ELW estimator whenever a nonzero mean or trend is likely.

5.3. Bandwidth Selection

The bandwidth parameter m is an important tuning parameter that must be selected by the researcher. Applied work typically adopts power rules $m = \lfloor n^\alpha \rfloor$ with α ranging from roughly 0.5 to 0.8, and $\alpha = 0.65$ has emerged as a practical standard (Shimotsu and Phillips, 2005; Shimotsu, 2010; Baum et al., 2020). Data-driven methods such as the bootstrap MSE minimization procedure of Arteche and Orbe (2017) can be used to estimate the optimal bandwidth for LW, though this procedure often suggests much larger bandwidths than power rules. We recommend carrying out a sensitivity analysis at multiple bandwidths,

[20]The distorting effect of deterministic components on local Whittle estimation of the memory parameter is analyzed in detail by Iacone (2010).

particularly when qualitative conclusions (e.g., $d < 1$ vs. $d \geq 1$) change with reasonable bandwidth choices.

5.4. Structural Breaks and Spurious Long Memory

For series prone to regime changes, researchers should consider structural breaks before interpreting a large estimate of d as long memory. Disentangling genuine long memory from spurious long memory faces difficulties in both directions: semiparametric estimators overstate d in the presence of breaks (Diebold and Inoue, 2001; Granger and Hyung, 2004), while conventional break tests (Bai and Perron, 1998, 2003) are not robust to long memory and over-detect breaks in its presence, so neither can be used on its own to test for the other.

Specialized tests have been developed to discriminate between the two. Shimotsu (2006) exploits the property that genuine long memory produces stable d estimates across sample splits. Ohanissian et al. (2008) test whether d is invariant to temporal aggregation, a property satisfied by true long memory but violated by spurious memory from breaks. Qu (2011) tests whether the low-frequency spectrum is consistent with a single memory parameter throughout the band of frequencies used in estimation, rather than the disproportionate power at the very lowest frequencies that a level shift or smooth trend would produce. Sibbertsen, Leschinski, and Busch (2018) develop a multivariate version of this test.

Once contamination is suspected, the next step is to determine the break points, but conventional break-detection procedures over-detect breaks under long memory (as noted above). Iacone et al. (2013, 2014) develop procedures to detect and date breaks that remain valid under fractional integration. An informal check is to re-estimate d separately within each regime. Although the mean is presumed constant within regimes, it is unknown, so a mean-robust estimator such as 2ELW may be appropriate. If the full-sample estimate is positive while the subsample estimates collapse to zero, this is consistent with spurious long memory generated by level shifts. If the subsample estimates instead remain positive and close to the full-sample value, genuine persistence may coexist with the shifts (Section 4.4).

As an alternative to testing for breaks, researchers can turn to estimators designed to be robust to level shifts, such as the trimmed log-periodogram estimator of McCloskey and Perron (2013) or the LWLFC estimator of Hou and Perron (2014). Among local Whittle estimators, LWLFC explicitly models low-frequency contamination from level shifts, though it is valid only for stationary processes with $d \in [0, 1/2)$.

The distinction between genuine and spurious memory carries directly into forecasting. When the long memory is genuine, modeling it explicitly through an ARFIMA specification can improve forecasts over covariance-stationary short-memory models (Granger and Joyeux, 1980; Bhardwaj and Swanson, 2006). Otherwise it should be avoided, since it imposes persistence that the series will not exhibit out of sample.

5.5. Multivariate Extensions

The memory estimates produced by the methods surveyed here are often used as inputs to a subsequent empirical analysis. In multivariate settings a natural next question is whether several fractionally integrated series exhibit common long-run behavior, a phenomenon known as fractional cointegration. Semiparametric procedures for detecting it and determining the cointegrating rank build directly on local Whittle estimation: Robinson and Yajima (2002) develop rank determination for stationary fractional systems, and Nielsen and Shimotsu (2007) extend the approach to the nonstationary range using the ELW estimator. Additionally, the univariate estimates considered here offer useful guidance on specification and starting values in parametric models, such as the fractionally cointegrated vector autoregressive model of Johansen (2008) and Johansen and Nielsen (2012). Extensions of local Whittle estimation to spatial, functional, and high-dimensional settings (Chen and Wang, 2017; Li, Robinson, and Shang, 2021; Baek, Düker, and Pipiras, 2023) likewise take univariate memory estimation as their point of departure. The contaminations emphasized above—unknown means, time trends, and structural breaks—carry over to the multivariate setting, where they can distort inference about the rank of fractional cointegration.

5.6. Summary of Recommendations for Empirical Work

First, we recommend that applied researchers visually inspect their time series data for obvious trends, level shifts, or regime changes that may influence the choice of estimator. Second, in light of the strengths and weaknesses of various local Whittle estimators, we recommend applying multiple methods to estimate d as a robustness check: agreement across methods with different robustness properties lends confidence, whereas disagreement is a caution that one or more methods' assumptions may not hold. Agreement does not guarantee correctness, however, since a common contamination such as persistent short-run dynamics can bias all methods together. Third, we recommend conducting a bandwidth sensitivity analysis across $\alpha \in \{0.5, 0.6, 0.65, 0.7, 0.8\}$. Researchers should also consider using the bootstrap MSE-optimal selection procedure of Arteche and Orbe (2017). Fourth, when estimators disagree or visual inspection suggests regime changes, apply formal break detection methods and robust estimation of d as described above.

6. Conclusion

This paper carries out a systematic evaluation of six local Whittle methods for estimating the memory parameter d, reproducing key Monte Carlo results from the literature and extending them with cross-method comparisons under short-run dynamics, unknown means, deterministic time trends, and non-Gaussian innovations. The simulations and the accompanying

empirical case studies document each estimator's characteristic failure modes.

As the preceding analysis shows, no single local Whittle estimator dominates in all settings. The ELW estimator attains the minimal asymptotic variance of $1/4$ under ideal conditions, but is sensitive to deterministic components. Tapered methods offer robustness to such components at the cost of increased variance and a more limited range of valid parameter values than ELW. The 2ELW estimator includes adaptive mean correction and detrending, also at the expense of the parameter range. Data-driven bandwidth selection for the exact estimators remains an open problem.

Our recommendations are based on combining existing theory with simulation evidence, and the diagnostics we suggest are informal. Because no single method is universally robust, we recommend computing several estimators with complementary strengths, matching the choice to the features one suspects in the data, and interpreting any disagreement among them in terms of possible contaminations.

References

Abadir, K. M., W. Distaso, and L. Giraitis (2007). Nonstationarity-extended local Whittle estimation. *Journal of Econometrics 141*, 1353–1384.

Andrews, D. W. K. and P. Guggenberger (2003). A bias-reduced log-periodogram regression estimator for the long-memory parameter. *Econometrica 71*, 675–712.

Andrews, D. W. K. and Y. Sun (2004). Adaptive local polynomial Whittle estimation of long-range dependence. *Econometrica 72*, 569–614.

Arteche, J. (2020). Exact local Whittle estimation in long memory time series with multiple poles. *Econometric Theory 36*, 1064–1098.

Arteche, J. and J. Orbe (2017). A strategy for optimal bandwidth selection in local Whittle estimation. *Econometrics and Statistics 4*, 3–17.

Baek, C., M.-C. Düker, and V. Pipiras (2023). Local Whittle estimation of high-dimensional long-run variance and precision matrices. *Annals of Statistics 51*(6), 2386–2414.

Bai, J. and P. Perron (1998). Estimating and testing linear models with multiple structural changes. *Econometrica 66*, 47–78.

Bai, J. and P. Perron (2003). Computation and analysis of multiple structural change models. *Journal of Applied Econometrics 18*, 1–22.

Baillie, R. T. (1996). Long memory processes and fractional integration in econometrics. *Journal of Econometrics 73*, 5–59.

Baillie, R. T., G. Kapetanios, and F. Papailias (2014). Bandwidth selection by cross-validation for forecasting long memory financial time series. *Journal of Empirical Finance 29*, 129–143.

Baum, C. F., S. Hurn, and K. Lindsay (2020). Local Whittle estimation of the long-memory parameter. *Stata Journal 20*(3), 565–583.

Beran, J. (1994). *Statistics for Long-memory Processes*. New York: Chapman & Hall.

Bhardwaj, G. and N. R. Swanson (2006). An empirical investigation of the usefulness of ARFIMA models for predicting macroeconomic and financial time series. *Journal of Econometrics 131*, 539–578.

Blevins, J. R. (2026). PyELW: Exact local Whittle estimation for long memory time series in Python. Working paper, The Ohio State University.

Brillinger, D. R. (1981). *Time Series: Data Analysis and Theory*. Holden-Day.

Caporale, G. M., L. A. Gil-Alana, and C. Poza (2022). Inflation in the G7 countries: persistence and structural breaks. *Journal of Economics and Finance 46*, 493–506.

Chen, K. and M. Wang (2017). Local Whittle likelihood estimators and tests for spatial lattice data. *Journal of Statistical Planning and Inference 191*, 25–42.

Diebold, F. X. and A. Inoue (2001). Long memory and regime switching. *Journal of Econometrics 105*(1), 131–159.

Frederiksen, P., F. S. Nielsen, and M. Ø. Nielsen (2012). Local polynomial Whittle estimation of perturbed fractional processes. *Journal of Econometrics 167*, 426–447.

García-Enríquez, J. and J. Hualde (2019). Local Whittle estimation of long memory: Standard versus bias-reducing techniques. *Econometrics and Statistics 12*, 66–77.

Geweke, J. and S. Porter-Hudak (1983). The estimation and application of long memory time series models. *Journal of Time Series Analysis 4*(4), 221–238.

Granger, C. W. J. and N. Hyung (2004). Occasional structural breaks and long memory with an application to the S&P 500 absolute stock returns. *Journal of Empirical Finance 11*(3), 399–421.

Granger, C. W. J. and R. Joyeux (1980). An introduction to long-memory time series models and fractional differencing. *Journal of Time Series Analysis 1*(1), 15–29.

Henry, M. (2001). Robust automatic bandwidth for long memory. *Journal of Time Series Analysis 22*, 293–316.

Henry, M. and P. M. Robinson (1996). Bandwidth choice in Gaussian semiparametric estimation of long range dependence. In P. M. Robinson and M. Rosenblatt (Eds.), *Athens Conference on Applied Probability and Time Series Analysis, Volume II: Time Series Analysis In Memory of E.J. Hannan*, pp. 220–232. Springer.

Hosking, J. R. M. (1981). Fractional differencing. *Biometrika 68*(1), 165–176.

Hou, J. and P. Perron (2014). Modified local Whittle estimator for long memory processes in the presence of low frequency (and other) contaminations. *Journal of Econometrics 182*(2), 309–328.

Hurvich, C. M. and W. W. Chen (2000). An efficient taper for potentially overdifferenced long-memory time series. *Journal of Time Series Analysis 21*(2), 155–180.

Iacone, F. (2010). Local Whittle estimation of the memory parameter in presence of deterministic components. *Journal of Time Series Analysis 31*, 37–49.

Iacone, F., S. J. Leybourne, and A. M. R. Taylor (2013). On the behavior of fixed-b trend break tests under fractional integration. *Econometric Theory 29*, 393–418.

Iacone, F., S. J. Leybourne, and A. M. R. Taylor (2014). A fixed-b test for a break in level at an unknown time under fractional integration. *Journal of Time Series Analysis 35*, 40–54.

Jensen, A. N. and M. Ø. Nielsen (2014). A fast fractional difference algorithm. *Journal of Time Series Analysis 35*(5), 428–436.

Johansen, S. (2008). A representation theory for a class of vector autoregressive models for fractional processes. *Econometric Theory 24*, 651–676.

Johansen, S. and M. Ø. Nielsen (2012). Likelihood inference for a fractionally cointegrated vector autoregressive model. *Econometrica 80*, 2667–2732.

Künsch, H. R. (1987). Statistical aspects of self-similar processes. In Y. V. Prokhorov and V. V. Sazanov (Eds.), *Probability Theory and Applications: Proceedings of the 1st World Congress of the Bernoulli Society*, Volume 1, pp. 67–74. De Gruyter.

Li, D., P. M. Robinson, and H. L. Shang (2021). Local Whittle estimation of long-range dependence for functional time series. *Journal of Time Series Analysis 42*(5-6), 685–695.

López de Prado, M. (2018). *Advances in Financial Machine Learning*. Wiley.

McCloskey, A. and P. Perron (2013). Memory parameter estimation in the presence of level shifts and deterministic trends. *Econometric Theory 29*, 1196–1237.

Nielsen, M. Ø. (2007). Local Whittle analysis of stationary fractional cointegration and the implied–realized volatility relation. *Journal of Business & Economic Statistics 25*(4), 427–446.

Nielsen, M. Ø. and P. H. Frederiksen (2005). Finite sample comparison of parametric, semiparametric, and wavelet estimators of fractional integration. *Econometric Reviews 24*, 405–443.

Nielsen, M. Ø. and K. Shimotsu (2007). Determining the cointegrating rank in nonstationary fractional systems by the exact local Whittle approach. *Journal of Econometrics 141*, 574–596.

Ohanissian, A., J. R. Russell, and R. S. Tsay (2008). True or spurious long memory? A new test. *Journal of Business & Economic Statistics 26*, 161–175.

Phillips, P. C. B. and K. Shimotsu (2004). Local Whittle estimation in nonstationary and unit root cases. *Annals of Statistics 32*(2), 656–692.

Qu, Z. (2011). A test against spurious long memory. *Journal of Business & Economic Statistics 29*(3), 423–438.

Robinson, P. M. (1995a). Gaussian semiparametric estimation of long range dependence. *Annals of Statistics 23*(5), 1630–1661.

Robinson, P. M. (1995b). Log-periodogram regression of time series with long range dependence. *Annals of Statistics 23*(3), 1048–1072.

Robinson, P. M. and M. Henry (1999). Long and short memory conditional heteroskedasticity in estimating the memory parameter of levels. *Econometric Theory 15*(3), 299–336.

Robinson, P. M. and M. Henry (2003). Higher-order kernel semiparametric M-estimation of long memory. *Journal of Econometrics 114*, 1–27.

Robinson, P. M. and Y. Yajima (2002). Determination of cointegrating rank in fractional systems. *Journal of Econometrics 106*, 217–241.

Shimotsu, K. (2006). Simple (but effective) tests of long memory versus structural breaks. Queen's Economics Department Working Paper 1101, Queen's University.

Shimotsu, K. (2010). Exact local Whittle estimation of fractional integration with unknown mean and time trend. *Econometric Theory 26*(2), 501–540.

Shimotsu, K. (2012). Exact local Whittle estimation of fractionally cointegrated systems. *Journal of Econometrics 169*(2), 266–278.

Shimotsu, K. and P. C. B. Phillips (2005). Exact local Whittle estimation of fractional integration. *Annals of Statistics 33*, 1890–1933.

Sibbertsen, P., C. Leschinski, and M. Busch (2018). A multivariate test against spurious long memory. *Journal of Econometrics 203*(1), 33–49.

Velasco, C. (1999). Gaussian semiparametric estimation for non-stationary time series. *Journal of Time Series Analysis 20*(1), 87–126.

Whittle, P. (1951). *Hypothesis Testing in Time Series Analysis*. Uppsala: Almqvist & Wiksells.

Wingert, S., C. Leschinski, and P. Sibbertsen (2020). Seasonality robust local Whittle estimation. *Applied Economics Letters 27*(18), 1489–1494.

A. Robustness of the Estimator Comparison

The recommendations in Section 5 are based on the cross-method comparison of Section 3, where the sample size, the form of the short-run dynamics, and the innovation distribution were all fixed. In this appendix, we consider robustness to these choices. We hold the overall simulation design of Section 3.1 fixed and vary, in turn, the sample size, the form of the short-run dynamics, and the innovation distribution. As before, each estimator is evaluated across the full d grid, including values outside the respective regions of validity.

A.1. Sensitivity to Sample Size

Tables 10 and 11 repeat the comprehensive comparison at $n = 250$ and $n = 1000$, halving and doubling the baseline sample size $n = 500$ while using the same $m = \lfloor n^{0.65} \rfloor$ bandwidth rule. The qualitative ranking of Section 3.1 is preserved at both sample sizes: ELW (and 2ELW within its range) remains valid and uniformly accurate across the full d grid, while the standard LW and LWLFC estimators continue to fail once d leaves their region of validity. Within each estimator's valid range, bias and MSE decline with n as expected. Overall, the patterns documented in the main text are stable across the sample sizes considered.

A.2. Sensitivity to the Short-Run Specification

In Table 12, we replace the AR(1) short-run component with an MA(1) component, simulating ARFIMA$(0, d, 1)$ processes with moving-average parameter $\theta \in \{0.5, 0.8\}$ at $n = 500$. (The baseline case $\theta = 0$ coincides with the $\rho = 0$ panel of Table 3 and is omitted.) Even though the MA(1) term results in a different spectral density shape near the origin, the overall contamination patterns carry over. The ordering of the estimators under MA(1) dynamics matches the AR(1) ordering, with the exact methods most accurate overall, the Velasco estimator carrying the largest bias among the valid methods, and LW and LWLFC failing outside their valid range. The effects are, however, milder by more than an order of magnitude: at $d = 0$ with $\theta = 0.8$ the ELW bias is only 0.015, compared to 0.416 for the AR(1) case at $\rho = 0.8$.

Finally, in Table 13 we consider ARMA(1,1) short-run dynamics over three specifications of increasing difficulty: $(\varphi, \theta) \in \{(0.5, 0.5), (0.8, 0.5), (0.9, 0.5)\}$, with the last being a near-unit-root case. This is a much more challenging design than in the main text: the ELW bias at $d = 0$ rises from 0.116 to 0.434 to 0.683 across the three configurations. The contrast with the negligible MA(1) effects indicates that the severity of short-run bias is governed by the proximity of the autoregressive root to unity, not by the particular short-run model. The range and failure structure are essentially preserved: at $d = 2.2$ under $(\varphi, \theta) = (0.9, 0.5)$ the LW and LWLFC estimators collapse toward the unit-root boundary (bias near -1.15), while

the exact methods continue to track d in the nonstationary region, displaced by the same uniform bias seen at central d. Short-run dynamics bias the estimators in unison, whereas mean or trend contamination drives ELW away from the tapered estimators.

A.3. Sensitivity to the Innovation Distribution

The experiments above all use Gaussian innovations, but many series to which these estimators are applied, such as asset returns, exhibit heavy tails and volatility clustering. Therefore, as a robustness check, we repeat the baseline ARFIMA$(0, d, 0)$ comparison with both $t(5)$ and GARCH(1,1) innovations, each standardized to have mean zero and unit variance. The GARCH(1,1) innovations satisfy $\varepsilon_t = \sigma_t \eta_t$ with $\sigma_t^2 = \omega + \alpha\varepsilon_{t-1}^2 + \beta\sigma_{t-1}^2$, $\eta_t \sim$ i.i.d. N$(0, 1)$, and $(\omega, \alpha, \beta) = (0.1, 0.1, 0.8)$, so that volatility is persistent ($\alpha + \beta = 0.9$). For the LW estimator, Robinson and Henry (1999) showed that conditional heteroskedasticity of this form leaves the N$(0, 1/4)$ limiting distribution unchanged.

The results, displayed in Table 14, indicate that the comparison of Section 3.1 does not depend on Gaussianity specifically. Relative to the Gaussian baseline (the $\rho = 0$ panel of Table 3), heavy-tailed $t(5)$ innovations (top panel) leave both bias and MSE essentially unchanged. The conditional heteroskedasticity of GARCH(1,1) innovations (bottom panel) likewise produces similar biases and only a slight increase in variance, consistent with the findings of Robinson and Henry (1999). The characteristic failure modes of the baseline are preserved in both panels: LW and LWLFC collapse toward the unit-root boundary for $d \geq 1.8$, and 2ELW fails under strong antipersistence.

TABLE 10. Estimator Comparison at $n = 250$

		Bias						MSE					
d	ρ	LW	V	HC	ELW	2ELW	LWLFC	LW	V	HC	ELW	2ELW	LWLFC
-2.2	0.0	1.387	0.050	0.828	-0.000	1.109	1.231	2.035	0.051	0.770	0.011	1.306	1.525
-1.8	0.0	0.907	0.025	0.446	0.000	0.724	0.817	0.917	0.049	0.248	0.011	0.571	0.672
-1.2	0.0	0.283	0.002	0.112	-0.002	0.278	0.233	0.119	0.048	0.030	0.011	0.099	0.060
-0.6	0.0	0.021	-0.016	0.036	-0.001	0.004	-0.018	0.012	0.048	0.018	0.011	0.010	0.015
-0.3	0.0	-0.003	-0.025	0.018	-0.001	-0.004	-0.038	0.011	0.049	0.017	0.011	0.011	0.017
0.0	0.0	-0.011	-0.029	0.006	-0.002	-0.002	-0.052	0.011	0.049	0.017	0.011	0.011	0.020
0.3	0.0	-0.011	-0.028	-0.002	-0.002	0.001	-0.075	0.011	0.050	0.017	0.011	0.011	0.032
0.6	0.0	-0.002	-0.022	-0.007	-0.001	0.016	-0.131	0.011	0.049	0.017	0.011	0.010	0.101
1.2	0.0	-0.128	-0.011	-0.012	-0.001	-0.001	-0.132	0.025	0.049	0.017	0.010	0.010	0.043
1.8	0.0	-0.723	0.022	0.004	-0.002	-0.002	-0.712	0.545	0.050	0.016	0.011	0.011	0.543
2.2	0.0	-1.151	0.056	0.047	-0.003	-0.003	-1.141	1.342	0.053	0.018	0.010	0.010	1.334
-2.2	0.5	1.223	0.234	0.769	0.154	1.047	1.206	1.596	0.103	0.655	0.035	1.155	1.455
-1.8	0.5	0.776	0.219	0.460	0.156	0.715	0.806	0.676	0.096	0.241	0.035	0.546	0.651
-1.2	0.5	0.299	0.192	0.254	0.157	0.303	0.272	0.110	0.086	0.081	0.035	0.106	0.082
-0.6	0.5	0.162	0.175	0.204	0.155	0.154	0.148	0.038	0.081	0.060	0.036	0.035	0.035
-0.3	0.5	0.150	0.171	0.192	0.157	0.155	0.137	0.033	0.077	0.054	0.035	0.035	0.032
0.0	0.5	0.144	0.168	0.180	0.156	0.157	0.130	0.031	0.077	0.050	0.035	0.035	0.030
0.3	0.5	0.141	0.167	0.170	0.154	0.161	0.119	0.030	0.077	0.047	0.035	0.038	0.031
0.6	0.5	0.148	0.171	0.167	0.156	0.159	0.099	0.033	0.079	0.045	0.035	0.035	0.060
1.2	0.5	-0.081	0.179	0.161	0.155	0.155	-0.080	0.023	0.081	0.044	0.035	0.035	0.025
1.8	0.5	-0.721	0.213	0.176	0.157	0.157	-0.713	0.545	0.093	0.047	0.035	0.035	0.543
2.2	0.5	-1.151	0.249	0.216	0.157	0.156	-1.143	1.344	0.111	0.062	0.035	0.035	1.337
-2.2	0.8	1.201	0.633	0.906	0.521	1.143	1.210	1.518	0.453	0.858	0.285	1.342	1.466
-1.8	0.8	0.826	0.617	0.710	0.523	0.843	0.831	0.722	0.431	0.522	0.286	0.734	0.696
-1.2	0.8	0.562	0.596	0.613	0.523	0.545	0.555	0.329	0.405	0.393	0.286	0.307	0.322
-0.6	0.8	0.515	0.582	0.582	0.522	0.521	0.513	0.278	0.389	0.358	0.286	0.285	0.276
-0.3	0.8	0.508	0.581	0.572	0.522	0.523	0.506	0.270	0.388	0.347	0.286	0.287	0.269
0.0	0.8	0.503	0.576	0.562	0.522	0.532	0.501	0.265	0.382	0.336	0.286	0.297	0.264
0.3	0.8	0.499	0.577	0.555	0.523	0.524	0.495	0.262	0.383	0.328	0.286	0.287	0.261
0.6	0.8	0.474	0.581	0.550	0.523	0.523	0.472	0.237	0.389	0.323	0.286	0.286	0.238
1.2	0.8	-0.021	0.592	0.545	0.522	0.522	-0.018	0.041	0.401	0.317	0.285	0.285	0.044
1.8	0.8	-0.720	0.621	0.557	0.522	0.521	-0.711	0.548	0.434	0.329	0.286	0.284	0.546
2.2	0.8	-1.152	0.637	0.584	0.522	0.520	-1.145	1.346	0.455	0.357	0.285	0.283	1.340

Notes: Monte Carlo results for ARFIMA$(1, d, 0)$ processes with $n = 250$, $m = 36$, 10,000 replications. Shaded cells indicate MSE > 0.05.
LW = Local Whittle, V = Velasco (Kolmogorov), HC = Hurvich–Chen, ELW = Exact Local Whittle, 2ELW = Two-step ELW, LWLFC = Local Whittle robust to low-frequency contamination.

TABLE 11. Estimator Comparison at $n = 1000$

		Bias						MSE					
d	ρ	LW	V	HC	ELW	2ELW	LWLFC	LW	V	HC	ELW	2ELW	LWLFC
-2.2	0.0	1.593	0.046	1.117	-0.001	1.266	1.295	2.617	0.016	1.321	0.004	1.668	1.710
-1.8	0.0	1.065	0.035	0.640	-0.002	0.795	0.829	1.208	0.015	0.466	0.004	0.682	0.695
-1.2	0.0	0.345	0.024	0.120	-0.003	0.257	0.224	0.156	0.014	0.025	0.004	0.080	0.054
-0.6	0.0	0.017	0.019	0.016	-0.002	0.002	-0.001	0.004	0.014	0.006	0.004	0.003	0.004
-0.3	0.0	-0.000	0.016	0.007	-0.001	-0.002	-0.015	0.004	0.014	0.006	0.004	0.004	0.004
0.0	0.0	-0.004	0.015	0.002	-0.002	-0.002	-0.022	0.004	0.014	0.005	0.004	0.004	0.005
0.3	0.0	-0.004	0.017	-0.002	-0.002	-0.001	-0.029	0.004	0.014	0.006	0.004	0.004	0.007
0.6	0.0	0.004	0.015	-0.006	-0.003	0.010	-0.049	0.004	0.014	0.005	0.003	0.003	0.017
1.2	0.0	-0.125	0.025	-0.006	-0.002	-0.002	-0.125	0.021	0.014	0.005	0.004	0.004	0.021
1.8	0.0	-0.745	0.048	0.005	-0.001	-0.001	-0.744	0.569	0.016	0.005	0.003	0.003	0.568
2.2	0.0	-1.168	0.064	0.028	-0.002	-0.002	-1.167	1.373	0.019	0.006	0.004	0.004	1.372
-2.2	0.5	1.401	0.122	0.997	0.065	1.150	1.208	2.038	0.029	1.062	0.008	1.383	1.461
-1.8	0.5	0.895	0.113	0.553	0.065	0.705	0.802	0.866	0.027	0.351	0.008	0.538	0.643
-1.2	0.5	0.274	0.102	0.144	0.066	0.255	0.220	0.096	0.024	0.027	0.008	0.076	0.050
-0.6	0.5	0.075	0.094	0.085	0.065	0.066	0.066	0.010	0.023	0.013	0.008	0.008	0.009
-0.3	0.5	0.065	0.093	0.078	0.065	0.065	0.058	0.008	0.023	0.012	0.008	0.008	0.007
0.0	0.5	0.062	0.092	0.073	0.065	0.065	0.054	0.007	0.022	0.011	0.008	0.008	0.007
0.3	0.5	0.062	0.094	0.070	0.065	0.066	0.052	0.007	0.023	0.011	0.008	0.008	0.007
0.6	0.5	0.069	0.093	0.066	0.065	0.070	0.050	0.009	0.023	0.010	0.008	0.008	0.012
1.2	0.5	-0.105	0.103	0.068	0.065	0.065	-0.105	0.019	0.024	0.010	0.008	0.008	0.020
1.8	0.5	-0.747	0.118	0.074	0.065	0.065	-0.747	0.572	0.028	0.011	0.008	0.008	0.572
2.2	0.5	-1.167	0.137	0.097	0.066	0.066	-1.167	1.372	0.033	0.015	0.008	0.008	1.371
-2.2	0.8	1.307	0.407	0.988	0.326	1.128	1.203	1.776	0.181	1.030	0.111	1.319	1.447
-1.8	0.8	0.841	0.399	0.608	0.326	0.746	0.804	0.752	0.175	0.393	0.111	0.579	0.647
-1.2	0.8	0.402	0.390	0.376	0.327	0.387	0.391	0.169	0.167	0.147	0.111	0.155	0.160
-0.6	0.8	0.327	0.383	0.352	0.325	0.325	0.327	0.111	0.162	0.130	0.110	0.110	0.111
-0.3	0.8	0.323	0.381	0.348	0.326	0.326	0.322	0.108	0.161	0.128	0.110	0.110	0.108
0.0	0.8	0.321	0.380	0.344	0.326	0.326	0.321	0.107	0.160	0.125	0.110	0.110	0.107
0.3	0.8	0.321	0.382	0.342	0.326	0.330	0.321	0.107	0.161	0.123	0.111	0.113	0.107
0.6	0.8	0.321	0.385	0.342	0.327	0.327	0.311	0.107	0.163	0.123	0.111	0.111	0.119
1.2	0.8	-0.054	0.388	0.339	0.326	0.326	-0.053	0.026	0.166	0.121	0.110	0.110	0.026
1.8	0.8	-0.742	0.401	0.344	0.327	0.326	-0.741	0.568	0.175	0.124	0.111	0.111	0.568
2.2	0.8	-1.165	0.415	0.358	0.326	0.326	-1.165	1.368	0.187	0.134	0.111	0.111	1.367

Notes: Monte Carlo results for ARFIMA$(1, d, 0)$ processes with $n = 1000$, $m = 89$, 10,000 replications. Shaded cells indicate MSE > 0.05.
LW = Local Whittle, V = Velasco (Kolmogorov), HC = Hurvich–Chen, ELW = Exact Local Whittle, 2ELW = Two-step ELW, LWLFC = Local Whittle robust to low-frequency contamination.

TABLE 12. Estimator Comparison under MA(1) Short-Run Dynamics

		Bias						MSE					
d	θ	LW	V	HC	ELW	2ELW	LWLFC	LW	V	HC	ELW	2ELW	LWLFC
-2.2	0.5	1.352	0.089	0.901	0.013	1.109	1.208	1.916	0.034	0.888	0.006	1.301	1.461
-1.8	0.5	0.872	0.076	0.483	0.014	0.694	0.803	0.835	0.032	0.281	0.006	0.527	0.645
-1.2	0.5	0.255	0.058	0.108	0.014	0.247	0.216	0.093	0.029	0.022	0.006	0.077	0.049
-0.6	0.5	0.029	0.047	0.040	0.013	0.016	0.006	0.007	0.029	0.011	0.006	0.006	0.008
-0.3	0.5	0.013	0.045	0.029	0.013	0.012	-0.006	0.006	0.029	0.010	0.006	0.006	0.008
0.0	0.5	0.008	0.042	0.020	0.013	0.013	-0.015	0.006	0.028	0.010	0.006	0.006	0.009
0.3	0.5	0.008	0.042	0.014	0.013	0.014	-0.027	0.006	0.028	0.010	0.006	0.006	0.012
0.6	0.5	0.018	0.044	0.010	0.014	0.028	-0.052	0.007	0.028	0.010	0.006	0.006	0.035
1.2	0.5	-0.120	0.056	0.008	0.012	0.012	-0.120	0.022	0.030	0.010	0.006	0.006	0.024
1.8	0.5	-0.737	0.083	0.022	0.014	0.014	-0.733	0.560	0.034	0.010	0.006	0.006	0.557
2.2	0.5	-1.161	0.109	0.054	0.013	0.013	-1.158	1.360	0.039	0.012	0.006	0.006	1.356
-2.2	0.8	1.317	0.087	0.878	0.014	1.091	1.204	1.819	0.034	0.846	0.006	1.260	1.451
-1.8	0.8	0.839	0.075	0.465	0.016	0.677	0.802	0.777	0.033	0.262	0.006	0.504	0.643
-1.2	0.8	0.245	0.060	0.106	0.017	0.242	0.215	0.087	0.031	0.021	0.006	0.074	0.048
-0.6	0.8	0.029	0.046	0.040	0.015	0.017	0.006	0.007	0.029	0.011	0.006	0.006	0.008
-0.3	0.8	0.015	0.044	0.030	0.015	0.013	-0.005	0.006	0.029	0.011	0.006	0.006	0.008
0.0	0.8	0.010	0.048	0.024	0.015	0.015	-0.013	0.006	0.029	0.010	0.006	0.006	0.009
0.3	0.8	0.011	0.044	0.017	0.016	0.017	-0.022	0.006	0.029	0.010	0.006	0.006	0.012
0.6	0.8	0.020	0.046	0.012	0.015	0.030	-0.049	0.007	0.028	0.010	0.006	0.006	0.036
1.2	0.8	-0.119	0.059	0.011	0.016	0.016	-0.118	0.021	0.029	0.010	0.006	0.006	0.022
1.8	0.8	-0.736	0.080	0.023	0.015	0.015	-0.732	0.559	0.033	0.010	0.006	0.006	0.557
2.2	0.8	-1.160	0.111	0.056	0.016	0.016	-1.157	1.358	0.039	0.013	0.006	0.006	1.354

Notes: Monte Carlo results for ARFIMA$(0, d, 1)$ processes with $n = 500$, $m = 56$, 10,000 replications. Shaded cells indicate MSE > 0.05.
LW = Local Whittle, V = Velasco (Kolmogorov), HC = Hurvich–Chen, ELW = Exact Local Whittle, 2ELW = Two-step ELW, LWLFC = Local Whittle robust to low-frequency contamination.

TABLE 13. Estimator Comparison under ARMA(1,1) Short-Run Dynamics

			Bias						MSE					
d	φ	θ	LW	V	HC	ELW	2ELW	LWLFC	LW	V	HC	ELW	2ELW	LWLFC
-2.2	0.5	0.5	1.209	0.210	0.842	0.117	1.044	1.201	1.544	0.072	0.777	0.020	1.151	1.442
-1.8	0.5	0.5	0.760	0.196	0.472	0.117	0.671	0.801	0.640	0.066	0.257	0.020	0.486	0.641
-1.2	0.5	0.5	0.261	0.179	0.193	0.115	0.268	0.236	0.085	0.059	0.047	0.019	0.083	0.059
-0.6	0.5	0.5	0.125	0.171	0.150	0.117	0.116	0.116	0.022	0.057	0.032	0.020	0.020	0.021
-0.3	0.5	0.5	0.113	0.164	0.138	0.116	0.115	0.105	0.019	0.054	0.029	0.020	0.020	0.018
0.0	0.5	0.5	0.110	0.167	0.133	0.116	0.117	0.101	0.018	0.055	0.028	0.020	0.020	0.018
0.3	0.5	0.5	0.110	0.163	0.126	0.116	0.118	0.099	0.018	0.054	0.026	0.020	0.021	0.018
0.6	0.5	0.5	0.116	0.169	0.122	0.116	0.119	0.084	0.020	0.055	0.025	0.019	0.020	0.036
1.2	0.5	0.5	-0.092	0.174	0.120	0.116	0.116	-0.091	0.020	0.057	0.025	0.020	0.020	0.020
1.8	0.5	0.5	-0.735	0.199	0.130	0.115	0.115	-0.732	0.559	0.067	0.027	0.019	0.019	0.557
2.2	0.5	0.5	-1.158	0.229	0.161	0.116	0.116	-1.155	1.355	0.079	0.035	0.020	0.020	1.351
-2.2	0.8	0.5	1.156	0.559	0.919	0.433	1.087	1.201	1.404	0.341	0.890	0.195	1.220	1.443
-1.8	0.8	0.5	0.778	0.548	0.636	0.434	0.778	0.808	0.642	0.330	0.421	0.196	0.626	0.653
-1.2	0.8	0.5	0.482	0.533	0.500	0.434	0.466	0.475	0.241	0.314	0.260	0.196	0.223	0.234
-0.6	0.8	0.5	0.432	0.523	0.477	0.434	0.433	0.431	0.194	0.304	0.239	0.196	0.195	0.194
-0.3	0.8	0.5	0.427	0.523	0.470	0.434	0.434	0.426	0.189	0.303	0.233	0.196	0.196	0.189
0.0	0.8	0.5	0.423	0.519	0.463	0.434	0.437	0.423	0.186	0.299	0.226	0.195	0.200	0.186
0.3	0.8	0.5	0.421	0.519	0.458	0.432	0.434	0.420	0.184	0.298	0.222	0.195	0.196	0.185
0.6	0.8	0.5	0.412	0.521	0.455	0.434	0.434	0.409	0.177	0.300	0.219	0.196	0.196	0.181
1.2	0.8	0.5	-0.037	0.529	0.453	0.433	0.433	-0.036	0.032	0.309	0.217	0.195	0.195	0.033
1.8	0.8	0.5	-0.732	0.550	0.460	0.434	0.434	-0.728	0.558	0.331	0.223	0.196	0.196	0.556
2.2	0.8	0.5	-1.160	0.569	0.481	0.434	0.433	-1.157	1.358	0.351	0.241	0.196	0.195	1.355
-2.2	0.9	0.5	1.182	0.803	1.039	0.681	1.163	1.204	1.448	0.675	1.113	0.472	1.379	1.450
-1.8	0.9	0.5	0.870	0.794	0.823	0.684	0.875	0.851	0.777	0.661	0.689	0.476	0.779	0.729
-1.2	0.9	0.5	0.701	0.783	0.741	0.684	0.688	0.700	0.499	0.644	0.561	0.476	0.481	0.498
-0.6	0.9	0.5	0.676	0.774	0.722	0.682	0.682	0.675	0.464	0.629	0.533	0.473	0.473	0.464
-0.3	0.9	0.5	0.672	0.771	0.717	0.683	0.686	0.672	0.460	0.625	0.525	0.474	0.479	0.460
0.0	0.9	0.5	0.670	0.776	0.714	0.683	0.686	0.670	0.457	0.632	0.521	0.474	0.478	0.456
0.3	0.9	0.5	0.665	0.773	0.709	0.684	0.685	0.662	0.449	0.627	0.515	0.475	0.477	0.450
0.6	0.9	0.5	0.611	0.775	0.705	0.684	0.684	0.612	0.383	0.630	0.509	0.475	0.476	0.384
1.2	0.9	0.5	-0.022	0.786	0.704	0.684	0.684	-0.019	0.047	0.646	0.508	0.476	0.475	0.048
1.8	0.9	0.5	-0.732	0.802	0.709	0.683	0.682	-0.728	0.559	0.670	0.515	0.475	0.473	0.557
2.2	0.9	0.5	-1.157	0.821	0.722	0.683	0.682	-1.154	1.354	0.702	0.531	0.474	0.472	1.351

Notes: Monte Carlo results for ARFIMA$(1, d, 1)$ processes with $n = 500$, $m = 56$, 10,000 replications. Shaded cells indicate MSE > 0.05.
LW = Local Whittle, V = Velasco (Kolmogorov), HC = Hurvich–Chen, ELW = Exact Local Whittle, 2ELW = Two-step ELW, LWLFC = Local Whittle robust to low-frequency contamination.

TABLE 14. Estimator Comparison under Heavy-Tailed and GARCH Innovations

	Bias						MSE					
d	LW	V	HC	ELW	2ELW	LWLFC	LW	V	HC	ELW	2ELW	LWLFC
Student-t(5) innovations												
-2.2	1.480	0.072	0.971	-0.002	1.176	1.258	2.291	0.032	1.029	0.006	1.457	1.606
-1.8	0.968	0.055	0.533	-0.004	0.738	0.824	1.026	0.029	0.343	0.006	0.596	0.687
-1.2	0.292	0.039	0.108	-0.001	0.259	0.228	0.124	0.028	0.024	0.006	0.085	0.057
-0.6	0.017	0.027	0.022	-0.003	0.001	-0.010	0.007	0.027	0.010	0.006	0.006	0.008
-0.3	-0.002	0.025	0.012	-0.002	-0.004	-0.024	0.006	0.027	0.010	0.006	0.006	0.008
0.0	-0.007	0.024	0.004	-0.002	-0.002	-0.032	0.006	0.027	0.010	0.006	0.006	0.010
0.3	-0.009	0.021	-0.004	-0.004	-0.003	-0.047	0.006	0.027	0.010	0.006	0.006	0.014
0.6	0.003	0.028	-0.005	-0.002	0.013	-0.078	0.007	0.027	0.010	0.006	0.006	0.045
1.2	-0.125	0.038	-0.008	-0.003	-0.003	-0.124	0.022	0.028	0.009	0.006	0.006	0.024
1.8	-0.736	0.065	0.005	-0.002	-0.002	-0.732	0.559	0.031	0.009	0.006	0.006	0.557
2.2	-1.161	0.091	0.040	-0.002	-0.002	-1.158	1.359	0.035	0.011	0.006	0.006	1.355
GARCH(1,1) innovations												
-2.2	1.489	0.072	0.984	-0.003	1.187	1.260	2.316	0.033	1.052	0.007	1.484	1.609
-1.8	0.986	0.056	0.545	-0.004	0.750	0.825	1.057	0.031	0.353	0.007	0.613	0.689
-1.2	0.314	0.036	0.111	-0.003	0.270	0.229	0.136	0.030	0.025	0.007	0.090	0.057
-0.6	0.018	0.026	0.022	-0.003	0.002	-0.009	0.008	0.028	0.011	0.007	0.006	0.009
-0.3	-0.003	0.025	0.012	-0.003	-0.005	-0.025	0.007	0.029	0.011	0.007	0.007	0.010
0.0	-0.007	0.022	0.004	-0.003	-0.002	-0.034	0.007	0.029	0.011	0.007	0.007	0.011
0.3	-0.008	0.018	-0.004	-0.003	-0.002	-0.048	0.007	0.029	0.011	0.007	0.007	0.016
0.6	0.003	0.027	-0.006	-0.002	0.012	-0.085	0.007	0.030	0.011	0.007	0.007	0.051
1.2	-0.124	0.039	-0.008	-0.004	-0.004	-0.124	0.022	0.029	0.011	0.007	0.007	0.026
1.8	-0.734	0.066	0.006	-0.002	-0.002	-0.730	0.558	0.032	0.010	0.007	0.007	0.555
2.2	-1.161	0.090	0.039	-0.002	-0.002	-1.158	1.360	0.036	0.012	0.007	0.007	1.356

Notes: Monte Carlo results for ARFIMA$(0, d, 0)$ processes with $n = 500$, $m = 56$, 10,000 replications, and mean-zero, unit-variance innovations ε_t. Student-t(5): $\varepsilon_t = \eta_t/\sqrt{5/3}$ with $\eta_t \overset{\text{iid}}{\sim} t(5)$ (kurtosis 9). GARCH(1,1): $\varepsilon_t = \sigma_t \eta_t$ with $\eta_t \overset{\text{iid}}{\sim} \mathrm{N}(0,1)$ and $\sigma_t^2 = \omega + \alpha\varepsilon_{t-1}^2 + \beta\sigma_{t-1}^2$, $(\omega, \alpha, \beta) = (0.1, 0.1, 0.8)$, implying unit unconditional variance and kurtosis ≈ 3.35. Shaded cells indicate MSE > 0.05.

LW = Local Whittle, V = Velasco (Kolmogorov), HC = Hurvich–Chen, ELW = Exact Local Whittle, 2ELW = Two-step ELW, LWLFC = Local Whittle robust to low-frequency contamination.

TABLE 15. Comparison of Velasco (1999) Tapers

	Bartlett ($p = 2$)			Cosine ($p = 3$)			Kolmogorov ($p = 3$)		
d	Bias	S.D.	MSE	Bias	S.D.	MSE	Bias	S.D.	MSE
−3.5	1.6231	0.3326	2.745	0.1254	0.1644	0.043	0.2207	0.1796	0.081
−2.3	0.2173	0.1734	0.077	0.0698	0.1644	0.032	0.0757	0.1648	0.033
−1.7	0.0279	0.1211	0.015	0.0515	0.1643	0.030	0.0542	0.1649	0.030
−1.3	0.0090	0.1203	0.015	0.0419	0.1642	0.029	0.0431	0.1648	0.029
−0.7	−0.0048	0.1200	0.014	0.0315	0.1640	0.028	0.0313	0.1645	0.028
−0.3	−0.0097	0.1201	0.015	0.0274	0.1636	0.028	0.0268	0.1640	0.028
0.0	−0.0111	0.1201	0.015	0.0258	0.1632	0.027	0.0255	0.1635	0.027
0.3	−0.0103	0.1201	0.015	0.0257	0.1629	0.027	0.0259	0.1631	0.027
0.7	−0.0051	0.1203	0.014	0.0281	0.1625	0.027	0.0296	0.1626	0.027
1.3	0.0170	0.1222	0.015	0.0410	0.1628	0.028	0.0432	0.1622	0.028
1.7	0.0485	0.1258	0.018	0.0722	0.1654	0.033	0.0597	0.1620	0.030
2.3	−0.1774	0.1410	0.051	0.2316	0.2010	0.094	0.1020	0.1636	0.037
3.5	−1.4529	0.1378	2.130	−0.3994	0.1041	0.170	−0.4160	0.1835	0.207

Notes: Comparison of three Velasco tapers, $n = 500$ observations from ARFIMA$(0, d, 0)$, $m = \lfloor n^{0.65} \rfloor = 56$ frequencies, 10,000 replications. Shaded cells indicate MSE > 0.05.

B. Comparison of Velasco Tapers

Table 15 compares the finite-sample performance of the three tapers considered by Velasco (1999), using the same Monte Carlo design as Table 1.[21] The results reflect the fundamental trade-off between bias reduction and variance inflation due to tapering. Within the range $d \in [-0.7, 0.7]$, all three tapers perform well. The Bartlett taper ($p = 2$) achieves the lowest variance with standard deviations around 0.120.

We can see the advantages of higher-order tapering in the nonstationary range. The order-three Kolmogorov taper retains low bias throughout $d \in [1.3, 2.3]$ and improves on the Bartlett taper at the top of this range, where its bias at $d = 2.3$ is 0.102 against −0.177 for Bartlett, though at the cost of increased variance, with standard deviations around 0.16, roughly 40% above the theoretical value of $\sqrt{3.01/4m} = 0.116$. The cosine bell tracks the Kolmogorov taper closely while both remain in range, but its order-one validity becomes apparent by $d = 2.3$, where its bias exceeds that of the Bartlett and Kolmogorov tapers. At still more extreme values such as $d = 3.5$, all three tapers break down well outside their valid ranges.

[21] We note that the cosine bell taper is labeled $p = 3$, but this denotes the frequency subsampling interval rather than the order of the taper, which is one.